Fabrication of Google-trackable colorimetric test strips for detecting water leakages

---

by

Zodidi Gcolotela

Dissertation submitted in fulfilment of the requirement for the degree

MASTER OF APPLIED SCIENCES

in

CHEMISTRY

in the

FACULTY OF APPLIED SCIENCES

of

DURBAN UNIVERSITY OF TECHNOLOGY

Supervisor : Prof P.S. MDLULI

Co-supervisor : Dr M. Mlambo

2020

PREFACE

This work was conducted in the Department of Chemistry, Durban University of Technology, Steve Biko Campus, Durban, South Africa The work was performed under the esteem supervision of Prof P.S Mdluli with the assistance of Dr M Mlambo.

DECLARATION

I, **Zodidi Gcolotela** hereby declare that:

This dissertation is wholly my own work, and that all the references to the best of my knowledge, are accurately reported.

This work has not been submitted for a degree at any other university.

This thesis does not contain text, graphs or tables copied from the internet unless specifically acknowledged, and the source being cited accordingly.

This thesis does not contain other people's information, diagrams and pictures or other data, unless particularly recognized as being sourced from different authors. Written sources have been cited, their words have been re-written yet the general data assigned to them has been referenced and their correct words have been utilized, their written work has been set inside quotes and referenced.

Ms. Z Gcolotela (Candidate)

Dr. PS Mdluli (Supervisor)

Dr. M Mlambo (Co-supervisor)

CONFERENCE ATTENDANCE AND JOURNAL PAPER SUBMITTED

JOURNAL PAPERS SUBMITTED ARISING FROM THIS STUDY

Zodidi Gcolotela[a], Stanley Chibuzor Onwubu[a], Sindisiwe Fortunate Muthwa[a], Phumlane Selby Mdluli[a.] 2019 Fabrication of smart phone based colorimetric device for detection of water leaks**,** *Water SA* (**Under review**).

ABSTRACTS ACCEPTED ARISING FROM THIS STUDY

Zodidi Gcolotela[a], Stanley Chibuzor Onwubu[a], Phumlane Selby Mdluli[a]. 2019. Fabrication of smart phone based colorimetric device for detection water leaks and pH. 4th interdisciplinary research, Durban, South Africa

Zodidi Gcolotela[a], Stanley Chibuzor Onwubu[a], Phumlane Selby Mdluli[a]. 2018. Design and fabrication of real-time trackable microfluidic device for detecting water leaks. 3rd interdisciplinary research. Durban, South Africa.

Zodidi Gcolotela[a], Stanley Chibuzor Onwubu[a], Phumlane Selby Mdluli[a]. 2018. Google analytical supported microfluidic strip as a potential tool for water leaks detection. 43rd SACI Convention. Pretoria, South Africa.

DEDICATION

Dedicated to my loving husband Mr Chinedu Blessed Obiechefu and my child Adaeze Purity Qhayiya Obiechefu. Your love and support inspired me to pursuit of excellence and the desire to learn more.

ACKNOWLEDGEMENTS

The completion of this dissertation was made possible through the support, encouragement and assistance from my family, friends and colleagues. Indeed, the recognition that this work may receive is not possible through sheer effort, but to all those who made it possible. I am particularly indebted to the following individuals:

Dr. Stanley Onwubu – for spending many hours supervising this dissertation. It was through his patience, consistent encouragement, enthusiasm, constructive criticism and insightful guidance throughout my study that I was able to complete this dissertation timeously.

Prof. Phumlane Mdluli– for your thoroughness in correcting and structuring this dissertation. Your deep knowledge in research methodology, your expertise in proofreading this dissertation was invaluable throughout this dissertation. I wholeheartedly thank you.

Dr. Mbuso Mlambo-through your efforts my academic writing has improved. Your expertise in proofreading this dissertation was invaluable throughout this dissertation.

My husband and my child – your support and understanding throughout this study without any complaints when I am not spending the weekends with you. I really appreciate your love you have shown me, and encouragements words when things get tough.

My church – your prayers were never in vain. Your consistent prayers and encouragement were the ointment that kept me going throughout this dissertation.

My Mother – My source of inspiration, the flame of your love, continual support and encouragement ignited me to persevere in writing this dissertation.

Finally, no acknowledgement would be complete without a wholehearted thanks to Amcor Flexibles Durban (AFD) for giving me financial support in pursuing my dream of Masters in Applied sciences.

ABSTRACT

South Africa is a water scarce country due to the shortage of rainfall. This scarcity is further exacerbated by the loss of water through leakage from faulty pipes. The consequence is the high amount of revenue lost through leakages and the negative health implication from water unavailability. Given this concern, it becomes highly imperative to address the water wastage through leaks by timely identifying and fixing household leaking pipes. While different method of detecting water leaks have been proposed in the literature, they are, however, expensive and difficult to implement. Hence, it is therefore sensible for South Africa to make use of leading leakage detection technology on pressurised systems, which can rapidly alert operators to leaks and breakages, and detect leaks in old, low-pressure reticulation systems. In the last decade, paper-based microfluidic device had become highly useful for environmental monitoring, health diagnosis, and food safety due to their simplicity, ease of use, and cheap application. This study is focused on the fabrication of a trackable microfluidic device (μPADs) to detect water leaks

A quantitative research approach and an experimental design were followed. The μPADs were prepared by printing patterns of wax (100 μm width) on the paper surface and melting the wax into the paper to form hydrophobic barriers and put on a hot plate for the wax to penetrate the paper. Solutions of lower to higher pH were also prepared and were introduced to the chlorophenol red test strips and a range of colours from yellow (lower pH) to purple (higher pH) were obtained. Colour change for chlorophenol paper is irreversible and is based on pH variation and not on the amount of water available in a solution. The optimised pH range was wider than the typical grayscale-based image analysis and was successful for a wide pH range of 2–12 measurements. The QR codes attached to the strips enable tracking to obtain the location from which a leakage was detected and this is done with the use of Google analytics which can tell real-time users from the website and their locations. The digital images obtained with the μPADs were analysed using the CIEL*a*b* colour system. The colour change was also validated using both spectroscopy and optical microscope.

The study has exhaustively demonstrated that the combination of digital image analysis and a microfluidic paper-based analytical device (μPADs) are highly effective for both quantitative and qualitative analysis, and thus useful for the detection of household water leaks.

ACRONYMS

uPADs	Microfluidic paper devices
AFD	Amcor Flexibles Durban
QR	Quick Response
PMDS	Polydimethylsiloxane
HCG	Human chorionic gonadotropin
CFU	Colony-forming unit
E. coli	Escherichia coli
L. monocytogenes	Listeria monocytogenes
ATP	Adenosine triphosphate
HRP	Horseradish peroxidase
DNA	Deoxyribonucleic acid
PEDs	Paper-based electrochemical devices
CL	Chemiluminescence
PC	Personal computer
CMOS	Complementary metal-oxide-semiconductor
AChE	Acetylcholinesterase

TABLE OF CONTENTS

PREFACE ii
DECLARATION iii
CONFERENCE ATTENDANCE AND JOURNAL PAPER SUBMITTED iv
DEDICATION v
ACKNOWLEDGEMENTS vi
ABSTRACT vii
ACRONYMS ix
TABLE OF CONTENTS x
LIST OF FIGURES xiii
LIST OF TABLES xv
CHAPTER ONE 1
INTRODUCTION 1
1.1 Background and context of the Study 2
1.2 Problem Statement 4
1.3 Aim of the Study 4
1.4 Research Objectives 4
1.5 Rationale/Significance of the Study 4
1.6 Assumptions 5
1.7 Delimitation 5
1.8 Structure of the Thesis 5
CHAPTER TWO 7
LITERATURE REVIEW 7
2.1 Water and sources of water leaks 8
2.1.1 Consequence of water leaks 9
2.2 Method of detecting water leaks 10
2.3 Microfluidic paper (µPADs) as a sustainable alternative for water leak detection 11
2.3.1 Applications of µPADs 11
2.3.1.1 µPADs used in health diagnostic 11
2.3.1. 2 µPADs used in environmental science 12
2.3.1.3 µPADs used in food safety 12

2.4 Fabrication of paper-based microfluidic device 13
2.5 Detection techniques using µPAD 15
2.5.1 Electrochemical detection 16
2.5.2 Chemiluminescence 16
2.5.3 Colorimetric Analysis 17
2.6 Indicators for µPADs detection techniques 18
2.6.1 Cobalt chloride 18
2.6.2 Chlorophenol red 23
2.7 Google analytics and applications 24
2.7.1 Quick Response code 25
CHAPTER THREE 27
RESEARCH DESIGN AND METHODOLOGY 27
3.1 Materials and Methods 28
3.2 Fabrication trackable microfluidic (µPAD) paper device 28
3.3 Preparation of indicators 29
3.3.1 Chlorophenol red 29
3.2.2 Preparation of Cobalt (II) Chloride 30
3.4 Humidity test 31
3.5 pH test on Chlorophenol red test strips 32
3.5.1 Verification of pH using plastic cuvette 33
3.5.2 Verification of pH using Lovibond colorimetric filter 34
3.5.3 Validation of the colour change using UV Spectrophotometer 35
3.5.4 Optical Electron Microscopic Observation of colour 35
3.6 Location 35
3.7 Google analytics 36
3.8 Leak detection test 36
CHAPTER FOUR 38
RESULTS AND DISCUSSION 38
4.1 Scanning Electron Microscopic Observation of the device 39
4.2 Stability of the fabricated microfluidic paper 40
4.2 Colour Absorbance versus pH 42
4.2.1 Image validation of the colour change and pH using Optical microscope 44
4.3 Leak detection test 44
4.3.1 Real-time measurement 48

4.4 Future works 54
Chapter Five 56
CONCLUSION AND RECOMMENDATION 56
5.1 Revisiting the research objectives 57
5.2 Recommendations 58
References 59
Appendix 66

LIST OF FIGURES

Figure 2. 1: Showing cobalt chloride change from (A) blue (B) pink Cobalt chloride hexahydrate. 19
Figure 2. 2: Showing cobalt chloride purple colour change with absorption of water 19
Figure 2. 3: Showing cobalt chloride final pink colour change with absorption of water 19
Figure 2. 4: Scheme for colour change of cobalt chloride 20
Figure 2. 5: Hexaaqua cobalt chloride complex 20
Figure 2. 6: Chain structure of $CoCl_2.2H_2O$. 21
Figure 2. 7: Structure of trans and cis-$[CoCl_2(H_2O)_4]$..... 21
Figure 2. 8: Electronic configuration for the d-orbitals $[Co(H_2O)_6]^{2+}$ 22
Figure 2. 9: Electronic configuration for the d-orbitals $[CoCl_4]^{2-}$..... 23

Figure 3. 1: (a) Xerox wax printer for paper printing, (b) fabricated chromatographic paper, (c) heated chromatographic paper in a hot plate(d)adding drops of chlorophenol indicator and drying overnight (e) Barcode attached on dried cholrophenol test strip 29
Figure 3. 2: Showing Chlorophenol (a) Soaked filter cholrophenol red (b) Oven dried test strip..... 30
Figure 3. 3: Showing Cobalt (II) Chloride (a) Soaked filter cholrophenol red (b) Oven dried test strip..... 30
Figure 3. 4: Showing humidity test at 0:59 am and at a temperature of 22°C: (A) before test (B) EQ 072; (C) after test..... 31
Figure 3. 5: Showing humidity test at 7:04 am and at a temperature of 18.3 °C: (A) before test (B) EQ 073; (C) after test..... 32
Figure 3. 6: Showing pH of test strips (A) acidic water; (B) basic water 33
Figure 3. 7: Showing the verification of pH (a) prepared pH solution, (b) cuvette colorimtric devices (c) filter paper..... 34
Figure 3. 8: Showing the pH reading using Lovibond filter (A) pH 4, (B) pH 5; (C) pH 6; and (D) pH 8..... 35
Figure 3. 9: Map of study location 36

Figure 3. 10: Showing (A) detection of leaking pipe; (B) Leak detection using colour grab App..... 37
Figure 3. 11: Schematic illustration of trackable analytical real time water detection device..... 37

Figure 4. 1: Showing (A) SEM images of chromatography paper (B) EDX elemental composition (1-before; 2-after indicator application) 40
Figure 4. 2: CIELab colour scheme of cholorophenol red strip at difference pH, (a) RBG curve (b) XYZ colourrimetri plot, (c) horse shoe shaped CIElab color scheme and (d) plot of the Lab values. 41
Figure 4. 3: Plot of (a) colour differences (b,c and d) plot of the ratio of red, green and blue colours from acidic to basic solution. 42
Figure 4. 4: Graph showing of colour change (a) CIEb lab; and (b) RGB values of water samples there were validated using spectrophotometric analysis. 43
Figure 4. 5: graph of absorbance at 572nm Vs pH..... 44
Figure 4. 6: Schematic illustration of traceable analytical real time water detection device..... 45
Figure 4. 7: Shows the number of request made by people to detect water leaks .. 46
Figure 4. 8: (a) Graph of absorbance at 572 nm and grayscale value against pH, (b) Plots of (a) RGB colour coordnates against pH value, (c) La*b* values against pH and (d) Plots of ΔE, hue and chroma vs pH 47
Figure 4. 9: Proposed design of michrofluidic strips for testing water leaks, where, (a) foldable paper chromatographic strips for testing fabricated with both Cobalt Chlorider and Chlorophenol Red, (b) proposed colour disk showing the change in colour of cobalt chloride by varying the concentration of water in %. 55
Figure 4. 10: Dried Chlorophenol red test strips (a) cuvette (b) paper (c) optical microscope..... 71
Figure 4. 11: Chlorophenol red test strips (a) RGB; and (b) CIElab 71

LIST OF TABLES

Table 2. 1: pH range of chlorophenol red 24

Table 4. 1: Readings of pH with 3drops indicator 44

Table 4. 2: Schematic illustration of Google analytics which can tell real-time users from the website and their locations. 48

CHAPTER ONE

INTRODUCTION

1.1 Background and context of the Study

Water supply systems play an extremely important role in providing quality drinking water to household consumers, agricultural purpose, and industrial usage (Cosgrove and Rijsberman 2014). However, water leakage and water loss from burst pipes poses a serious threats to uninterrupted water supply (Yazdekhasti *et al.* 2018). This has a dire consequence to the quality of life, hygiene and health of hundreds or even thousands of inhabitants (Cosgrove and Loucks 2015). Moreover, and as pointed out by Pfister *et al.* (2017) water is one of the vital and scarce resources of life. In South Africa, this water scarcity is made even worse by the amount of municipality supplied water being lost through leaking or burst pipes and dripping taps. This is highly concerning from an economy perspective, as the leaks and pipe burst cost municipalities a lot of money. For instance, it is estimated that water loss due to burst pipes or water leakages cost eThekwini municipality approximately R710.90 million annually (Meyer 2017). Equally concerning, the recent water scarcity and drought being experience in Western Cape (Cassim 2018), called for an urgent need for an effective management of water supply in South Africa.

Despite these concerns, Hay *et al.* (2012) in their asserted views highlighted that water losses are very high in many towns in South Africa and no effective strategies are in place or developed by the municipalities to effectively address water losses. Consequently, du Plessis (2017) moots that a clear understanding of the real potential for reducing water losses are needed before measures adopted or implemented to avoid costly and ineffective demand management strategies. They proposed that such water management measures must be both cost effective and ultimately effective in implementing water conservation and water demand management measures, targets and structures. Therefore the detection, locating and correcting of water leakages on time would help in minimising water loss, fix the problem, saves water and money (Seyoum *et al.* 2017). Unfortunately, in many South African towns and locations the infrastructure needed to adequately monitor water leaks is either non-existent or inadequate (Hay *et al.* 2012).

As a consequence of the above, there is an urgent need for a proactive investment in the country's existing infrastructures, and programme that is aimed to reduce the water leakages along the full cycle – from treatment plant to tap. Hence, it is therefore sensible for South Africa to make use of leading leakage detection

technology on pressurised systems, which can rapidly alert operators to leaks and breakages, and detect leaks in old, low-pressure reticulation systems. Traditionally, detecting and identifying of water leaks in household levels require the analysis of different type of censored data in the household piping system. Seyoum *et al.* (2017), however, noted that this method is expensive and difficult to implement. Equally worth mentioning is many leaks at the domestic level contribute significantly to unaccounted-for water in many water distribution networks. This, Seyoum *et al.* (2017) noted are minor but numerous, thus may go unnoticed by the traditional monitoring techniques. This present study therefore reports on the use of a simple, inexpensive microfluidic paper device (µPADs) equipped with trackable device for the detection of water leaks.

Meredith *et al.* (2016) reported that a low-cost microfluidic paper-based analytical device (µPADs) offer an opportunity to tackle environmental need by increasing the frequency and geographic coverage of environmental monitoring while also reducing analytical costs and complexity of the measurement. Equally important, the fabrication of µPADs is relatively simple requiring the use of conventional inkjet printing techniques that involves paper-sizing agents (Jayawardane, McKelvie and Kolev 2015). In recent years, µPADs have gained numerous attention amongst researchers for its ability to sense multiplex analytes, rapid sample analysis, confirming diagnostic tests results, and reduction in the volume of samples (Lim, Goh and Khor 2017). Owing to these unique attributes, µPADs have been successfully used in the quantification of ammonia in wastewater (Jayawardane, McKelvie and Kolev 2015); blood separation (Songjaroen *et al.* 2012); glucose detection (Liu, Su and Ding 2016); quantification of particulate chromium (Rattanarat *et al.* 2013); detection of small size molecules (Busa *et al.* 2016); determination of nitrite in saliva (Bhakta *et al.* 2014); and detection of disease biomarkers (Lim, Goh and Khor 2017). Despite these, there is limited evidence in the use of µPADs for the monitoring of water leakage in South Africa. This study, therefore, aim to combine chemistry with technology by fabricating a colorimetric test strip that will help in detecting the leaks and alerting the municipality on time.

1.2 Problem Statement

Water leakage and water loss from burst pipes poses a serious threats to uninterrupted water supply (Yazdekhasti *et al.* 2018). This has a dire consequence to the quality of life, hygiene and health of hundreds or even thousands of inhabitants (Cosgrove and Loucks 2015). Moreover, and as pointed out by Pfister *et al.* (2017) water is one of the vital and scarce resources of life. In South Africa, water scarcity is made even worse by the amount of municipality supplied water being lost through leaking or burst pipes and dripping taps. This is highly concerning from an economy perspective, as the leaks and pipe burst cost municipalities a lot of money(Meyer 2017).

In attempting to address water leakages, this study will use a simple, inexpensive microfluidic paper device (µPADs) equipped with trackable device for the detection of water leaks. Meredith *et al.* (2016) reported that a low-cost microfluidic paper-based analytical device (µPADs) offer an opportunity to tackle environmental need by increasing the frequency and geographic coverage of environmental monitoring while also reducing analytical costs and complexity of the measurement.

1.3 Aim of the Study

The aim of this study was to fabricate a trackable microfluidic device to detect water leaks.

1.4 Research Objectives

The study research objectives are:

1.4.1.1 To design and fabrication of microfluidic device using chromographic paper to detect water leaks

1.4.1.2 To optimised and standardise the time, concentration and the volume of the indicator.

1.4.1.3 To develop a real-time Google analytical device to track water leaks.

1.5 Rationale/Significance of the Study

South Africa is amongst the dry and water scarce countries in the world. As such, South Africa is considered as a water stress country with limited portable water and

erratic rainfalls. Despite these concerns, Hay *et al.* (2012) in their asserted views highlighted that water losses are very high in many towns in South Africa and no effective strategies are in place or developed by the municipalities to effectively address water losses. Consequently, du Plessis (2017) moots that a clear understanding of the real potential for reducing water losses is needed before measures adopted or implemented to avoid costly and ineffective demand management strategies. They proposed that such water management measures must be both cost effective and ultimately effective in implementing water conservation and water demand management measures, targets and structures. Therefore the detection, locating and correcting of water leakages on time would help in minimising water loss, fix the problem, saves water and money (Seyoum *et al.* 2017). Unfortunately, in many South African towns and locations the infrastructure needed to adequately monitor water leaks is either non-existent or inadequate (Hay *et al.* 2012)

1.6 Assumptions

The following assumptions are made in relation to this study:

- Fabricated trackable microfluidic (µPAD) paper device is affordable and suitable for the detection of water leak.
- Google maps and the QR codes used are accurate and efficient to locate the area of interest.

1.7 Delimitation

Regardless of many locations, that could be located using this Technology in South Africa, this study will be limited in scope to two cities namely: Durban (KwaZulu-Natal province) and Johannesburg (Gauteng).

1.8 Structure of the Thesis

The thesis is divided into five chapters. Chapter one explicates the context of the study by detailing the reasons for developing trackable microfluidic device to detect water leaks. This directed the chapter towards the aim and objectives, hypothesis, assumptions, delimitations and scope of the study.

Chapter 2 presents an overview of the literature on chlorophenol red and microfluidic paper.

Chapter 3 describes the research design and methodology by detailing the quantitative research paradigm and experimental research design that is to be adopted in this study.

Chapter 4 presents the results on leak detection and Trackability. Tables, maps and images will support the analytical results. Overall, this chapter will provide a discussion on the fabricated microfluidic device to detect and to track water leaks NAM a by comparing to the current system used by municipalities.

Chapter 5 forms the final chapter and will provide the conclusions drawn from the study. It will also identify any limitations and consider future directions for this research.

CHAPTER TWO

LITERATURE REVIEW

This chapter reviews literature related to the current methods used to detect water leakages and explain their accessibility and cost. Subsequently, microfluidic paper and its uses will be discussed. Overall this literature review is structured into four sections. Section One discusses water and the sources of water leaks. Here, the consequence of water leaks will be detailed. Section Two discusses the methods of detecting water leaks in household water supply channel. Section Three introduces microfluidic devices and the advantage of paper base microfluidic device. It is projected that this will help to support the development of the trackable microfluidic device for leak detection as an alternative material to current ways of leak detection. Section Four described in detail the method of fabricating microfluidic device. Section Five highlights the method of detection using microfluidic with a particular emphasis on colorimetric methods. The chapter concludes with the evaluation of the role of information technology in modern science. Here, the use of Google analytical as a real-time monitoring trackable device for early water detection was discussed.

2.1 Water and sources of water leaks

According to Li and Qian (2018), water is an essential commodity as it plays an important role in the world economy. Equally important, water remain an indispensable resources for the well-being of human race as it is critical for the production and sustainability of food as well as household needs (Brauman *et al*. 2016). Despite the importance of water, the amount of clean water readily available for both domestic and industrial use are limited, and thus needs to be conserved to ensure its continuous supply (Kumar *et al.* 2017).

However, much of the water distributed for both domestic and industrial usage is lost through leaking pipes and dripping taps (Mavundla 2016). Furthermore, leaks may occur in domestic home appliances like the water coolers, washing machines, dehumidifiers, and dishwashers. More so, hot water heaters, faucets, water pipes, in-line water filters, and valves are other sources of domestic water leaks (Lu 2014). Apart from the aforesaid, it is noted that the moistures accumulated in the ventilation units or air conditioners condensation could be an indication of water leaks. As such, identifying dampness in these areas are highly advantageous in water leak detection applications (Lu 2014).

Added to this, water leaks that occur out of sight and in discrete places like in walls, attics, behind cabinets, etc. are, however, unnoticed until there is an accumulation of water which may constitute huge water loses (Bertran 2018).

2.1.1 Consequence of water leaks

From an economic perspective, water leakage could lead to financial constraints. As a consequence, businesses particularly property owners tend to insure their properties in an event of damage caused by water leaks (Meyer 2016). For those having larger commercial or residential buildings, the sky rocketing costs of insurance premiums presents a major concern and challenges. This is due to the undesirable consequences of water leaks in residential dwellings and commercial buildings that involves many residential apartments, units, and or office.

Moreover, it has been reported in the literature that water leaks can result to a significant damage to structure of building in commercial and or residential properties if undetected (Meyer 2016). From an economic point of view, failures to detect leaks timely may accumulate huge economic cost in thousands of rands from repairing the damages cause by water (Meyer 2016). Beside this, Mavundla (2016) claimed that 40% of the municipality supplied water is lost through leaking, dripping or burst pipes resulting to an estimated economic loss of more than R7-billion annually.

Apart from economic loss, and from health and safety context, an undetected water leak is a source of risk to the occupants of the building health. Unresolved water leaks, for instance, may result in the formation of hazardous microorganisms such as fungus spreading rapidly to the surrounding areas of the apartment (Bertran 2018). More so, leaks that goes unnoticed could rapidly spread from one apartment to another thereby causing considerable damage other areas (Farley *et al.* 2001; Meyer 2016). This may result to structural damaged thereby increasing the risk of collapse. Given the economic and health risk associated with water risk, it is of critical importance that leaks be detected immediately in order to reduce losses and its anticipated consequence. The next section will, therefore, explore the methods of detecting water leaks.

2.2 Method of detecting water leaks

In an attempt to address the quick response time needed to detect water leaks, several types of water leak detection devices have been proposed. Some of these devices include localised leak detection devices that are situated throughout various locations within a building to alert the presence of water have been previously investigated (Kates 2007). Such devices typically include a small housing enclosing both a water sensor and audible alarm. Doumit and Lynch Jr (2003), however, points out that the drawback of such devices is that an individual observer must be in arms' length from the detecting device to hear the audible alarm, thus making it impractical for remotely monitoring water leaks.

In attempt to address the abovementioned drawbacks, more sophisticated water leak detection systems have been designed to meet the on-going needs of efficiently monitoring and detecting water leaks. Amongst these technological improvements, include automated water systems. Puust *et al.* (2010) revealed that automated water detection systems generally include a controller having a number of status indicators, and a plurality of water detection sensors electrically connected to the controller. According to the authors, the indicators generally include a plurality of light emitting diodes or LED segment blocks that provide a visual indication of the operative location of water sensors. However, and like the localised water leak detection, the automated systems suffer a number of drawbacks (Doumit and Lynch Jr 2003; Hill and Sullivan 2008). For instance, automated water leak detection systems are difficult to install, provide limited remote observation of conditions, and are limited in application (Meyer 2016).

Furthermore, it is reported in the literature that automated water leak detection systems are not integrated or in continuous communication with a remote system that is supervised or monitored by an agency (Meyer 2016). Given this concern, and in agreement with Lu (2014), it is important to develop a water leak detection system that is easy to install and integrate, provides exact point identification of water leak detection sensors, and is user friendly. As such, Lu (2014) advocated for a water leak detection system that has a centralized detection control and are in remote communication to a central monitoring agency. According to his view, such a system could provide continuous monitoring, immediate notification, and point identification

data of water leaks. Cognisance of this will be taken into consideration when developing and designing a water leak detection device using a microfluidic paper.

2.3 Microfluidic paper (µPADs) as a sustainable alternative for water leak detection

According to Ballerini, Li and Shen (2012), µPADs offer a wide variety of advantages, such as price, easy storage and transportation, and are easily disposable. It also offers the advantage that it requires no external pumping as paper naturally wicks fluid via capillary action. Moreover, paper is a universally available porous material made up of cellulose fibres. Owing to this, µPADs has the ability to store reagents in active form within the fibre network. The cellulose in the paper is naturally hydrophilic, which allows the penetration of aqueous solutions; thus providing a solid foundation to use paper as a microfluidic system to replace the glass and polydimethylsiloxane (PDMS) devices (Ríos, Zougagh and Avila 2012). The next section will provide a considerable highlight of the extensive application of µPADs devices.

2.3.1 Applications of µPADs

This section detailed both the environmental, health, and food safety applications of µPADs devices. The researcher envisaged that the wealth of empirical evidence on the advantage of its use will provide motivation for its application in the detection of water leaks.

2.3.1.1 µPADs used in health diagnostic

Due to its simplicity and ease of use, µPADs have found numerous applications including in health diagnostic (Hassan and Syaza 2018). The early work of Kang *et al.* (1997) reported that µPADs has been used in health diagnostics, and that the first medical device was made from paper in 1956 to detect glucose in urine through a colour change from yellow to green. According to the authors, if the paper turned green, glucose was detected in the urine (positive result), if the colour remained yellow, no glucose was detected in the urine (negative result). Their report revealed that µPADs paper was soaked in glucose oxidase, catalase and horseradish peroxidise and the result read from a colour chart after 1min of been dipped in the sample and this test is still routinely done in modern day science for the diagnosis of

diabetes type I and type II. Currently, at the forefront of paper devices are the dipstick and lateral flow assays such as the home pregnancy testing kit (Hassan and Syaza 2018), and malaria testing kit (Mthembu *et al.* 2017). The reportedly use of µPADs paper in healthcare may be related to the fact that the device could afford a helpful and rapid response to a patients test sample (Hassan and Syaza 2018).

2.3.1. 2 µPADs used in environmental science

Microfluidic paper has also been used in environmental sciences, particularly for the detection of hydrogen sulphide (H_2S) (Kato Jr *et al.* 2011), and ammonia compounds in water (Nxumalo 2019). For H_2S test for example, the microfluidic paper is appropriate to detect the compounds in drinking water derived from surface water, boreholes for faecal contamination, and rain water sources. For detecting H_2S, the paper test strip used are common laboratory reagents. This can be achieved by adding a measured amount of a common household liquid detergent and "boiled" water to the reagents. Thereafter, the solution is impregnated on a piece of absorbent paper and dried in a low-temperature oven. The dried paper strip is placed in a clear small plastic or glass bottle or tube. A water sample is collected in the container containing the reagents and stored in the dark at room temperature for about 3 days. If the sample contains hydrogen sulphide producing organisms, the pad and water turn black. The black colour and the rotten egg smell of hydrogen sulphide clearly indicate that there is a problem. With such an indicator it is not difficult to convince uneducated villagers that the water may not be safe to drink (Mosley and Sharp 2005; Gupta *et al.* 2008).

With reference to its use in ammonia detection, a recent study (Nxumalo 2019) demonstrates the use of µPADs to effectively detect and quantify the presence of ammonia in waste water. According to her report, the analytical quantification has a limit of detection 3.37 mg L-1 and 3.20 mg L-1, and a colour change of yellow and green were based on the analytical reagents. The author conclusively suggests that the waste water samples results obtained were similar to those measured with a spectrophotometric method.

2.3.1.3 µPADs used in food safety

Another important application of is in the food industry. Busa (2016) noted that paper-based approach for food safety monitoring is attractive because it is simple to

use, and it is of low-cost. Hence, using µPAD, onsite detection of foodborne contaminants is achievable.

Jokerst *et al.* (2012), for example, reportedly used µPADs for micro spot detection of *Escherichia coli* (*E. coli*) O157:H7, *Listeria monocytogenes* (*L. monocytogenes*) and *Salmonella Typhimurium* in ready to eat meat samples. The aforementioned pathogens were collected from foods by a swab sampling technique and cultured in media before adding to a chromogen-impregnated paper-based well device. A colour change was observed indicating the presence of an enzyme associated with the pathogen of interest and detection was achieved (Jokerst *et al.* 2012). According to the authors report, the developed µPAD was capable of detecting pathogenic bacteria in ready-to-eat meat (bologna) at a concentration of as low as 101 CFU mL´1 within 12 h or less, which is significantly less time than the gold standard method (requires several days) for bacterial detection and enumeration (Jokerst *et al.* 2012).

Similarly, Jin *et al.* (2015) reported on the detection of Salmonella via adenosine triphosphate (ATP) using µPAD. The authors observe a colour change using the µPAD only when ATP is present which suggest the presence of Salmonella in the sample. The above aforementioned studies indicate that µPAD could be applied for food and water monitoring.

2.4 Fabrication of paper-based microfluidic device

The fabrication of paper-based microfluidic diagnostic devices consists of selectively hydrophobic paper using cellulose reactive hydrophobic agents. Li *et al.* (2010) revealed that the hydrophilic–hydrophobic contrast of patterns created has excellent ability to control capillary penetration of aqueous liquids in paper channels. According to the authors, a new method of fabricating microfluidic devices that is paper-based can be established using digital ink jet printers. This is because bio-chemical sensing zones can easily be formed using ink jet printing by delivering biomolecules and indicator reagents into the patterns of the device with precision (Xia *et al.* 2016). This method thus allows the complete sensor, i.e. channel patterns and the detecting chemistries, to be fabricated only by two printing steps (Li *et al.*

2010). Sensors can be fabricated for specific tests, or they can be made as general devices to perform on-demand quantitative analytical tasks by incorporating the required detection chemistries for the required tasks. Owing to this, fabrication method can be scaled up and adapted to use high speed, high volume and low-cost commercial printing technology.

Papers derived from cellulose fibres are hydrophilic in nature, and this enables aqueous liquids to penetrate within the paper fibre matrix. Owing to this property, many attempt have been made to fabricate microfluidic systems using paper (Stock and Rice 1974; Li, Tian and Shen 2010; Khan *et al*. 2016). It has been reported that paper-based microfluidic devices can be built by demarcating hydrophilic paper by walls of hydrophobic polymers (Martinez *et al.* 2007). Following this principle, Martinez *et al.* (2007) explored the use of a photolithography method to create microfluidic channels in a paper by making hydrophobic barrier walls in the paper matrix. Hydrophobic photoresist polymers provide a very good physical barrier, which defines the liquid penetration pathways into a paper. A liquid sample can be similar to the barrier concept since they rely on cellulose fibres in the paper to be physically covered by a layer of hydrophobic materials.

Furthermore, the microfluidic device present a novel possibilities whereby analytes in a liquid sample can be simultaneously detected. Thus making it well suited for making health care and telemedicine devices. The fabrication process, however, has two main drawbacks. Firstly, the photoresist barrier becomes hardened making it prone to damage from bending and folding. The second drawback is that multiple steps is required for photolithography fabrication process. Thus necessitating the need for an expensive equipment. To overcome the aforementioned drawbacks, an alternative and more efficient process of fabrication becomes highly important.

In another method, a modified plotter was used to create a barrier pattern. As reported by Bruzewicz *et al.* (2008), this is achieved by printing polydimethylsiloxane (PDMS) onto paper. This method overcame the problem of physical inflexibility of devices made using photolithography. However, the quality of the barrier definition deteriorated, since the penetration of PDMS in the paper could not be very well controlled, resulting in the wall of the barrier not being straight. This method is also limited to producing devices on an up-graded scale and at a high speed. Abe *et al.*

(2008) took a polymer (polystyrene) solution impregnation approach to introduce hydrophobicity into the paper matrix. They then used a micro drop dispensing device to print solvent onto the impregnated paper to dissolve the polymer and to form fine liquid penetration channels. These researchers also printed chemical sensing agents into their pattern to form a functional device for biomedical detection.

Lu *et al*. (2009) used a wax printer to generate microfluidic patterns in paper. The pattern was then heated to allow wax diffusion into paper and to form the barriers for microfluidic channels. These fabrication concepts are the motivation of this work is to present a new concept of creating microfluidic patterns and channels by generating a hydrophilic–hydrophobic contrast on the paper surface, forming liquid penetration channels, rather than building patterns using a physical polymer barrier. Building barriers in the paper to define channels is a limiting process to the speed and cost of large-scale fabrication, as it usually involves multiple steps including polymer impregnation and pattern development.

Of interest, the ink jet printing approach reported in this study can fabricate paper-based microfluidic patterns in a single printing step. This concept, therefore, has a clear potential to enable the fabrication of paper-based microfluidic sensors, i.e. patterns and incorporated sensing chemistries, by continuous high-speed and large-volume industrial printing processes. Such efficiencies enable the ultimate practical use of these sensors for health care and environmental applications.

2.5 Detection techniques using µPAD

There are three main areas of detection best suited for paper microfluidic devices which is constantly been upgraded, renewed and retested to allow for the most accurate method to be utilised (Xia, Si and Li 2016). According to Xia, Si and Li (2016), this allows for both quantitative analysis (data which can be measured numerically) and qualitative analysis (data which relies on observation and interpretation) to be performed. The use of digital result taken from many paper microfluidic devices already available for qualitative analysis (Nxumalo 2019). This and together with the use of Image J provides a numerical measurement of the analytes of interest according to the density of a colour change (Xia, Si and Li 2016).

Dungchai, Chailapakul and Henry (2009) suggest that the use of Image J to quantitatively measure the digital images provide more accurate than qualitative measurement. It is worth mentioning that Image J was used in this study to generate quantitative measurement of the colour change intensity. Accordingly, and given the benefits of quantitative assessment, different techniques have been proposed in literature for the quantitative detection of data when using µPADs (Dungchai, Chailapakul and Henry 2009). Amongst these techniques, the electrochemical chemiluminescence and colorimetric detection have developed much interest because they are simple to use and well understood for most applications. The aforesaid techniques will be taken into consideration when using µPADs in the detection of water leaks.

2.5.1 Electrochemical detection

Electrochemical detection is characterised by low cost, portability, simplicity, high selectivity, good sensitivity, low electrical power consumption, and minimal instrumentation(Dungchai, Chailapakul and Henry 2009). As a result, it is eminently suitable for µPADs and has led to the emergence of a new class of µPADs device known as “paper-based electrochemical devices” (PEDs) (Hasanzadeh and Shadjou 2016). The electrochemical systems employed in these PEDs involve microelectrodes, convective mass transfer, surface-modified electrodes, flow injection, signal amplification, ion-selective electrodes, and ion-exchange membranes. Moreover, the electrochemical techniques coupled to these devices include cyclic voltammetry, amperometry, coulometry, and potentiometry (Oh and Chow 2015).

2.5.2 Chemiluminescence

Another detection technique that has also generated research interest for µPADs due to its inexpensive reagents is the chemiluminescence (CL) (Liu *et al.* 2015; Xu *et al.* 2016). CL is characterised by a high signal-to noise ratio, and hence low limits of detection are potentially achievable. Equally, and in conjunction with immunoassays, CL measurement is routinely performed nowadays for the determination of trace biomedical analytes such as tumor marker proteins on a microtiter plate (Xu *et al.* 2016). Though this method remains an effective method for analysis in paper

microfluidic devices it can however be improved by the addition of an electrochemical detection.

2.5.3 Colorimetric Analysis

Colorimetric methods that are based on image analysis of the device of digital images are most commonly used as they are simple and easy to operate (Cate *et al.* 2014; Liu, Yang and Liu 2019). Such methods require no special instrument or apparatus, only a digital camera or a smartphone (Nxumalo 2019). Additionally, they allow quantitative analysis by reading out the colour information red, green and blue region (RGB) value or cyan, magenta, yellow, black (CMYK) value of the detection area of a μPADs in the digital image. The RGB colour model is device dependent and the colour information is obtained as separate RGB colour coordinates. CIEL*a*b* colour system is a device independent and has three colour coordinates L indicating lightness, a* coordinates where +a indicates red and –a* indicates green and b* coordinates where +b indicates yellow and –b indicates blue. Komatsu et. al demonstrated a quantitative analysis based on multiple colour changes on μPADs using the CIEL*a*b* colour system to analyse the digital images (Komatsu *et al.* 2016). Kim *et al.* (2017) reported a smartphone-based optical platform for colorimetric analysis of μPADs.

Hossain and his co-worker studied a lab-in-a-phone: smartphone-based portable fluorometer for pH measurements of environmental water (Hossain *et al.* 2015). Image analysis and μPADs are a suitable combination for the point of care applications and testing in resource limited locations. The mean of RGB values (grayscale) is one of the most common condition in image-analysis based Colorimetry (Shen 2003; Komatsu *et al.* 2016). However, the grayscale does not allow quantitative analysis based on multiple changes of colour such as a universal pH test strip because the grayscale cannot follow multiple colour changes (Komatsu *et al.* 2016).

Colour difference is a measurement of the numerical differences between colour specifications and is given by the following equation:

$$\Delta E = \sqrt{(\Delta L)^2 + (\Delta a)^2 + (\Delta b)^2} \qquad (1)$$

Chromaticity or chroma is the saturation level or intensity of a particular hue and is defined as the distance of departure of a chromatic colour from the neutral (grayscale) colour with the same value. Chroma is the dullness or vividness of colour and is given by equation (2). Hue angle is defined as the attribute by which we distinguish red from green, blue from yellow, etc and is given by equation (3).

$$C^* = \sqrt{(a)^2 + (b)^2} \quad (2)$$

$$\mathrm{h} = tan^{-1}(\frac{b^*}{a^*}) \quad (3)$$

where:

a denotes red/green value, b denotes red/green value

h denotes the Hue angle (angular measurement) and C specifies Chroma

This study, therefore, aim to combine chemistry with technology by fabricating a colorimetric test strip that will help in detecting the leaks and alerting the municipality on time. Thus, report a simple colorimetric pH measurement method using a µPADs based on the CIEL*a*b* colour space.

2.6 Indicators for µPADs detection techniques

One of the characteristics of the µPADs is that it functions through colour change. Hence, the selection of appropriate indictors for its use becomes highly relevant. As revealed in the literature, cobalt chloride and chlorophenol red are the most widely used indicators (American Chemistry Council 2006; Damaceanu, Sava and Constantin 2016).

2.6.1 Cobalt chloride

Cobalt chloride, $CoCl_2$, is a fascinating compound that changes colour in response to humidity (American Chemistry Council 2006; Damaceanu, Sava and Constantin 2016). As humidity increases, cobalt chloride changes colour from sky blue to purple to pink (Figure 2.1). As highlighted in the American Chemistry Council (2006) report, the striking changes in colour make cobalt chloride useful as a humidity indicator in weather instruments.

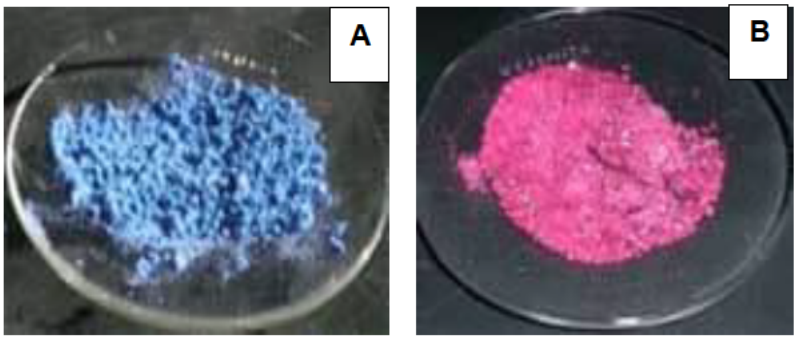

Figure 2. 1: Showing cobalt chloride change from (A) blue (B) pink Cobalt chloride hexahydrate.

More so, and from a chemistry perspective, it is noted that as the humidity increases, and water is absorbed by $CoCl_2$, the crystal structure rearranges itself to make room for water molecules (Figure 2.2).

$$\underset{\text{(blue)}}{CoCl_2 + 2\,H_2O} \rightarrow \underset{\text{(purple)}}{CoCl_2 \bullet 2\,H_2O}$$

Figure 2. 2: Showing cobalt chloride purple colour change with absorption of water

Firstly, it is observe that the two water molecules present surround each cobalt atom, thus forming a purple colour solution dehydrate (Figure 2.3).

$$\underset{\text{(purple)}}{CoCl_2 \bullet 2\,H_2O} + 4\,H_2O \rightarrow \underset{\text{(pink)}}{CoCl_2 \bullet 6\,H_2O}$$

Figure 2. 3: Showing cobalt chloride final pink colour change with absorption of water

As the humidity increases further, the crystal structure again changes, this time rearranging itself to let four more water molecules surround each cobalt atom, forming the hexahydrate. As contain in the report by American Chemistry Council (2006) cobalt chloride has a crystalline structure that changes as the molecules shift to make room for water molecules. Consequently, this results to the colour change that makes cobalt chloride ideal for detecting the presence of water. Heating the hydrated forms of cobalt chloride reverses the reactions above, returning cobalt

chloride to the blue, water-free, or anhydrous, state. Water is "liberated" in these reactions, known as dehydration reactions (American Chemistry Council 2006).

The colour of Cobalt complexes changes with the coordination and the type of solvent used. The octahedral complexes of cobalt are pink coloured whilst the tetrahedral complexes are blue coloured. Cobalt structure rearranges, first the purple dihydrate, $CoCl_2.2H_2O$, forms and then at higher humidity the pink hexahydrate $CoCl_2.6H_2O$ is the product. Aqueous solutions of both $CoCl_2$ and the hydrate contain the species $[Co(H_2O)_6]^{2+}$. They also contain chloride ions. In the solid state $CoCl_2 \cdot 6H_2O$ consists of the molecule trans-$[CoCl_2(H_2O)_4]$ and two molecules of water of crystallization (Wells 1984) This species dissolves readily in water and alcohol. Concentrated aqueous solutions are red at room temperature but become blue at higher temperatures (The Merck Index 1960). $CoCl_2 \cdot 6H_2O$ is deliquescent, and the anhydrous salt $CoCl_2$ is hygroscopic, readily converting to the hydrate.

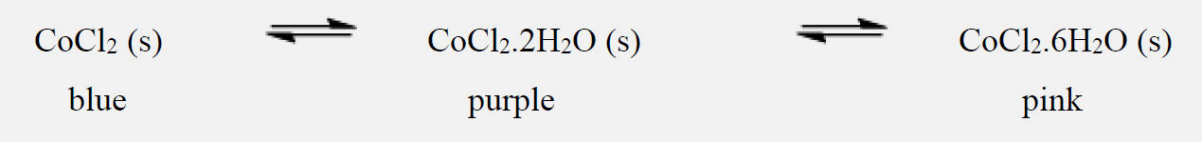

Figure 2. 4: Scheme for colour change of cobalt chloride

If the $CoCl_2.6H_2O$ as shown in Figure 2.5 below is gently heated up to 150°C - it gradually loses water forming the violet $CoCl_2.2H_2O$, then blue anhydrous $CoCl_2$. This can again be reversed by adding water. However, it was noted in this study that this mechanism is very sensitive to moisture thus was not suitable for this study.

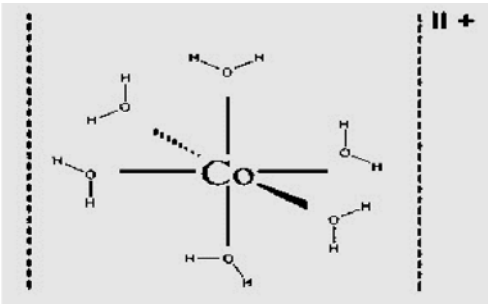

Figure 2. 5: Hexaaqua cobalt chloride complex

Cobalt can be used to make an indicator paper, similar to a litmus paper but containing cobalt chloride, which changes colour from blue to pink in the presence of

water. $CoCl_2.2H_2O$ has a chain structure in which each cobalt atom is bound to 4 bridging chlorides and two water molecules.

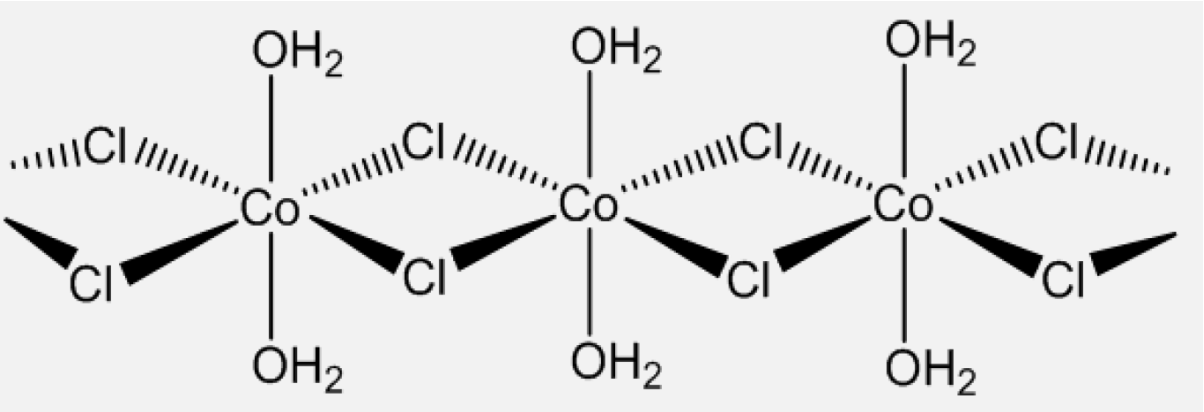

Figure 2. 6: Chain structure of $CoCl_2.2H_2O$.

$CoCl_2.6H_2O$ contains trans-$[CoCl_2(H_2O)_4]$ molecules, with two molecules of 'water of crystallisation' in the lattice, this can be written as $[CoCl_2(H_2O)_4].2H_2O$. Crystallisation of cobalt chloride around 50ºC would give tetrahydrate $CoCl_2.4H_2O$, which contains cis-$[CoCl_2(H_2O)_4]$ molecules as shown in Figure 2.7 below.

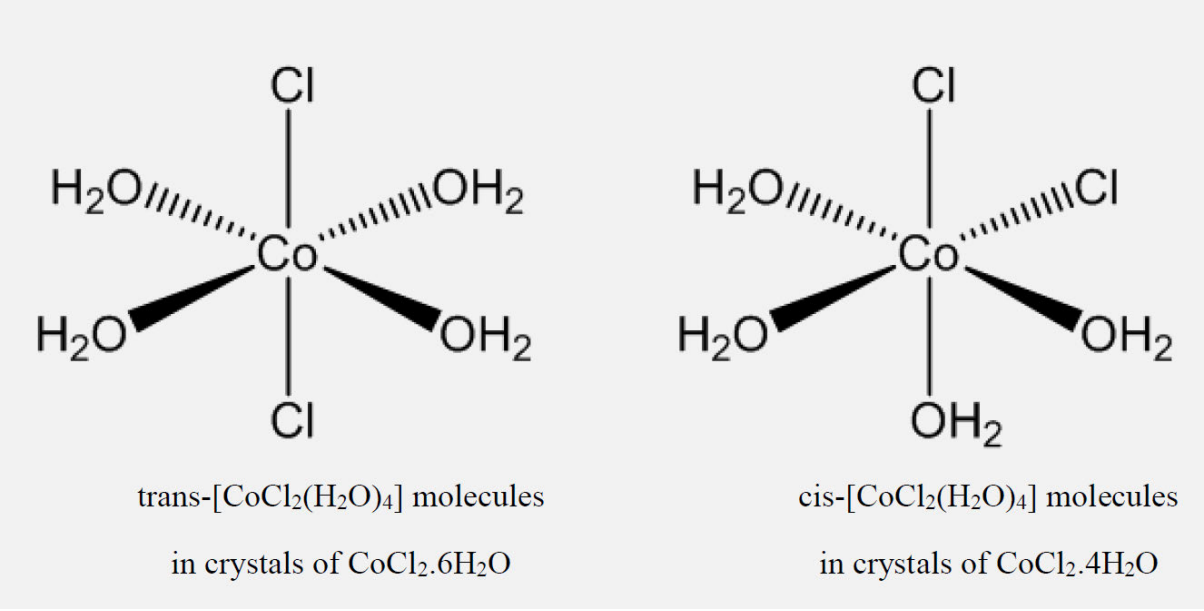

Figure 2. 7: Structure of trans and cis-$[CoCl_2(H_2O)_4]$

Normally the bulky chloride ligands stay as far apart as possible in the coordination sphere. In the tetrahydrate $CoCl_2.4H_2O$, it appears that hydrogen bonds between chlorides and the hydrogen atoms in water molecules in the next $CoCl_2(H_2O)_4$ molecule along make the cis structure more favourable.

Furthermore, the structure of $CoCl_2(H_2O)_4$ molecule can be explained using ligand-field theory (Britz *et al.* 2019). The colour of transition metal complexes is due to electronic transitions between different d-orbitals. Water produces larger splitting between the energy levels than chloride (H_2O is a 'stronger-field' ligand than Cl) so the energy differences between different electronic energy levels are smaller in complexes with lots of chlorides as ligands, so this has a significant effect on the colour.

Most transition metals generally form octahedral complexes, the coordination number of the metal is largely dictated by how many donor atoms can fit around the central metal. Crossing the d-3 transition series of the periodic table, the nuclear charge increases, but the screening due to filled electronic shells stay the same. This draws the outer electrons in closer, The octahedral complex of $[Co(H_2O)_6]^{2+}$ has the following electronic configuration for the d-orbitals (Figure 2.8)..

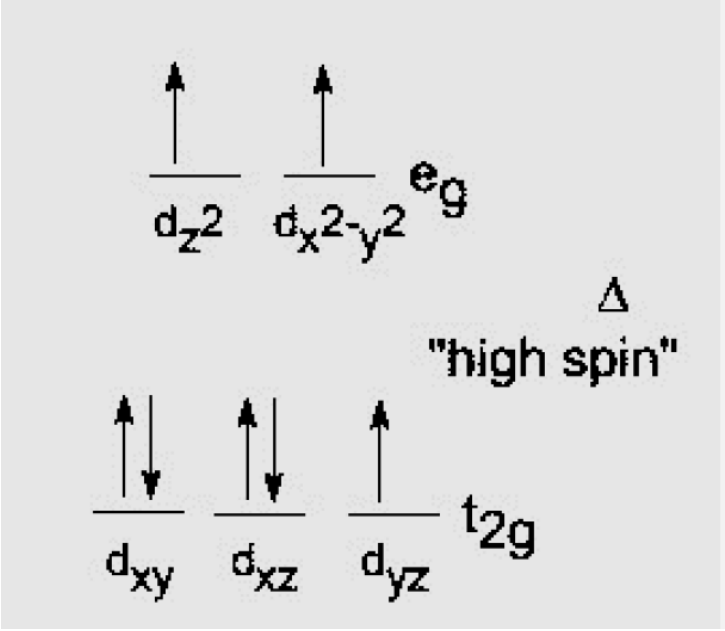

Figure 2. 8: Electronic configuration for the d-orbitals $[Co(H_2O)_6]^{2+}$

In the case of Cobalt (II), the energy splitting of the d-orbitals is small and is a high-spin complex (three unpaired electrons); the low-spin complex has one unpaired

electron. The difference in CFS-energy (Crystal Field Stabilization) of the octahedral and tetrahedral complex is small. With stronger ligands than water, the coordination changes from octahedral to tetrahedral.

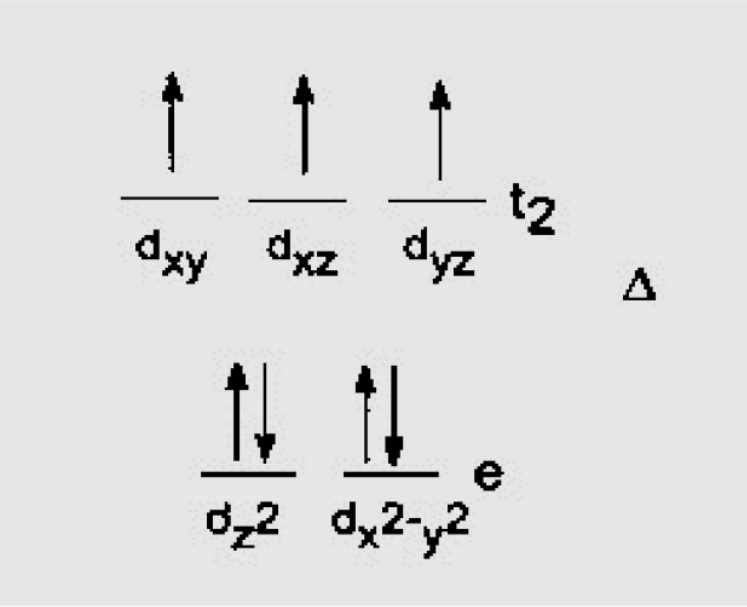

Figure 2. 9: Electronic configuration for the d-orbitals $[CoCl_4]^{2-}$

Firstly, Co(II) can exist in a tetrahedral environment as $[CoCl_4]^{2-}$ where there is no centre of symmetry and hence the d-d transitions are allowed whereas in an octahedral environment (such as in $[Co(H_2O)_6]^{2+}$] there is a centre of symmetry and d-d transitions forbidden by the selection rule (absorptivity is smaller) and hence colour is paler. The difference in colour is due to the ligands involved and the difference in eg-t_{2g} energy gaps in the case of tetrahedral and octahedral environments. The complexes are therefore blue in the case of chloride and pink in the case of water in this case.

If both complexes are octahedral, the colour is due to different ligands. If one of the ligands has pi-bonding, then Ligand to Metal Charge Transfer may take place which leads to much more intense colours because transitions are between pi and pi* orbitals which are allowed in terms of the selection rules.

2.6.2 Chlorophenol red

Chlorophenol red is a pH indicator, a kind of chemical that changes colour when the pH (acidity or alkalinity of the solution in it) goes up or down. Unlike some pH indicators, chlorophenol red changes colour at the same pH regardless of the

concentration of the solution. And according to McCrady (1995) it is important for accuracy. Phenol red in chlorophenol red exists as a red crystal that is stable in air. A solution of phenol red is used as a pH indicator, often in cell culture. Its colour exhibits a gradual transition from yellow (λ_{max} = 443 nm-) (Saha and Mukherjea 2015) to red (λ_{max} = 570 nm (Mills and Skinner 2011) over the pH range 6.8 to 8.2. As illustrated in Table 2.1, the phenol red turns a bright pink colour at a pH above 8.2

Table 2. 1: pH range of chlorophenol red

Phenol red (pH indicator)		
below pH 6.8		*above pH* 8.2
6.8	⇄	**8.2**

2.7 Google analytics and applications

Science and technology have increased significantly in recent years and collaborated in inventing new machines like smartphones, laptops, iPods etc. This increase in technology has spread to chemistry as well. As noted in the literature, there are several research area in chemistry where technology and chemistry have been intertwined using Google analytics (Fitzpatrick, Battilocchio and Ley 2016). Moreover, Google analytics is the most widely used website statistics service. For example, in 2012 survey, it was found that around 55% make use of it out of the 10,000 most popular websites (Mayer and Mitchell 2012). Another market share analysis claims that Google analytics is used at around 49.95% of the top 1,000,000 websites as ranked in 2010. In August 2013, Google analytics was used by 66.2 of the 10,000 most popular websites ordered by popularity as reported by BuiltWith (Sandhya and Kakulapati 2018).

More importantly, and of a particular interest to this study, Google analytics is a free web analytics offered by Google that tracks and reports website traffic, currently as a platform inside the Google marketing platform brand. Given that it is free to use, it was not surprising that it is the desired service among small blogs and national brands alike (Clifton 2012). For instance, Einstein (2016) disclosed that popular taxi

hailing service brand like Uber utilises the technology to drive their business model. This is achieved through the use of via smartphone connect driver-partners and riders which detect the exact location of the rider using Google analytics.

The Virgin group is another big brand that has found the usefulness of Google analytics. Calo and Rosenblat (2017) revealed that the Virgin groups find Google analytics extremely helpful in looking at the cross-pollination of its products. Samsung is able to track analytics to see which of its products are generating buzz, and is able to use this information to change around page displays and relative importance of each of its phones and other products on the landing page (Heath 2014).

Drawing from the above wide and useful application of Google analytics technology in solving daily human challenges, this study envisage to leverage the technology for a rapid onsite detection and communication of household water leaks to the relevant municipality. Essentially, the interplay between science and technology comes into play in fabrication of a trackable water leak strip as a cost effective and fast way to detect water leaks by attaching a Quick Response (QR). The QR codes attached to the strips will ultimately enable tracking to obtain the location from which a leakage was detected. This can easily be done with the use of cell phones that is connected to Google analytics. Ultimately, this can tell real-time users from the website and their locations. The next section discusses the Quick response code and its relevance in this study.

2.7.1 Quick Response code

QR codes were first invented by the Japanese where they are very common, and can be read quickly by a mobile smartphone. In terms of its popularity and wide acceptability, the QR codes may be seen in a magazine advert, on a billboard, a web page or even on someone's t-shirt. Once it is scanned on the user smartphone, it can provide exact details about that business (allowing users to search for nearby locations), or details about the person wearing the t-shirt, etc. (Rouillard 2008). The reason why they are more useful than a standard barcode is that they can store more date, including url links, geo coordinates, and text. The other key feature of QR codes is that many modern smartphones can scan them without requiring a chunky

hand –held scanner (Walsh 2010). This is highly critical to the present study. In addition, it is noted that in order to scan a QR code, the user need open the app, point the camera at the code and you are done. There is no need to take a photo or press a button, the app will automatically recognize any code your camera is pointing at (Wu and Xiong 2013).

In summary, the above chapter had exhaustively provided the motivation for the need to develop a simple device for the detection of water leaks. The chapter had highlighted the health and economic consequences of water leak. While different technologies was proposed in past, the chapter clearly presents their various drawbacks. Consequently, this leads to the need for an alternative technology that is simple, cheap, and easy to use. The microfluidic paper-based device readily comes to mind. It wide application both in healthcare and environment highly support its intended use for detecting water leaks. Overall, the chapter conclusively suggest that integration of science and technology through the use of Google analytics will present an innovative way of addressing water leaks. The next section will present the research methodology and design.

CHAPTER THREE

RESEARCH DESIGN AND METHODOLOGY

This chapter details the research design used in this study. The preliminary study that was conducted will first be described, particularly highlighting the fabrication of the water leak detection device. Subsequently, the methodology used in the main study, that is the various experimental work and analyses that were conducted, will be described in-depth.

3.1 Materials and Methods

Chlorophenol red (CAS number 4430-20-0), Cobalt (II) Chloride, Sodium Hydroxide were purchased at Nexor chemicals. All chemicals were of analytical grade and was used as purchased.

3.2 Fabrication trackable microfluidic (μPAD) paper device

Patterns of wax were printed on chromatographic paper using a wax printer. The paper was then heated on hot plate melting the wax to form hydrophobic barriers (Figure 3.1). A drop of the prepared chlorophenol red solution was introduced into hydrophilic circles of wax patterns of chromatographic paper and left to dry overnight. A Quick Response code (QR code) was generated using an online QR code generator and was used to encode and decode field test results. QR codes were printed and attached to the chromatographic paper (chlorophenol red test strip) and the top side covered with a clear cello tape to protect paper from tearing.

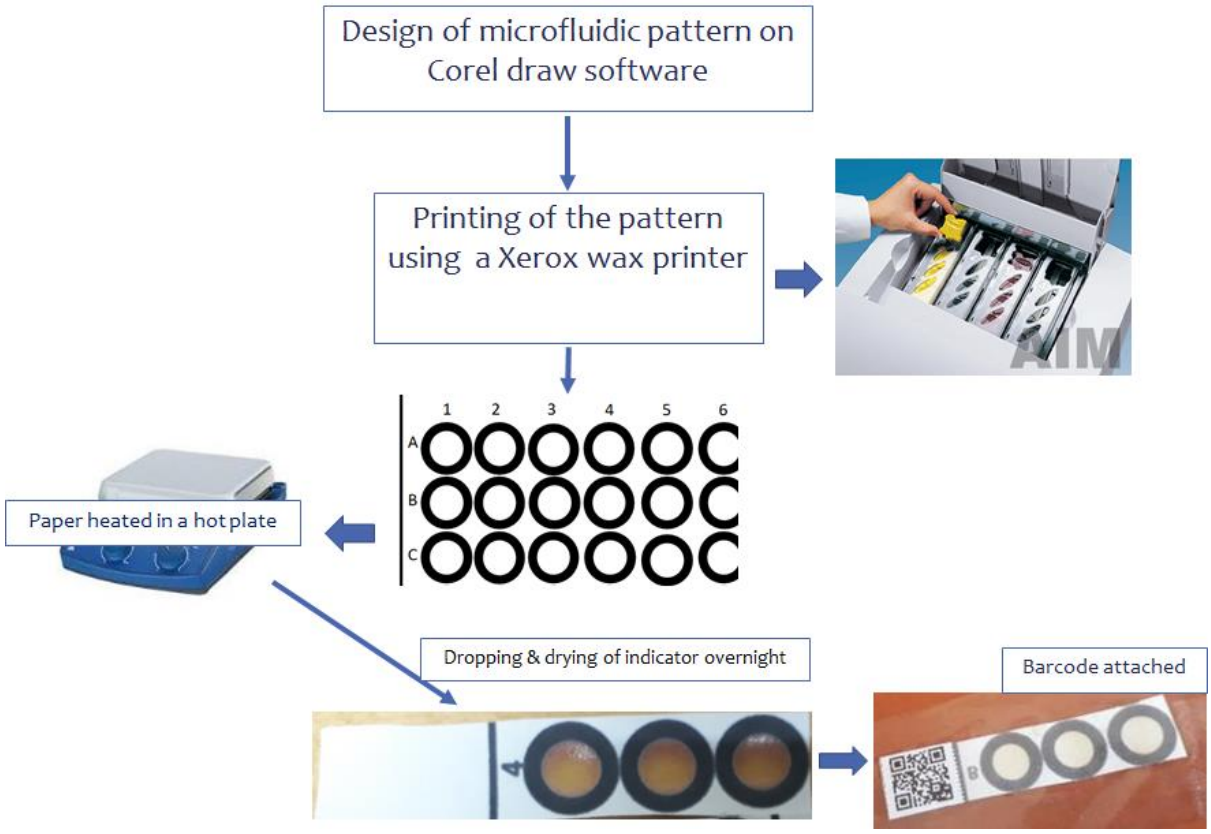

Figure 3. 1: (a) Xerox wax printer for paper printing, (b) fabricated chromatographic paper, (c) heated chromatographic paper in a hot plate(d)adding drops of chlorophenol indicator and drying overnight (e) Barcode attached on dried cholrophenol test strip

3.3 Preparation of indicators

To help establish the preferable indicator, the colorimetric test strips were prepared using Cobalt chloride and Chlorophenol red separately. These are detailed below.

3.3.1 Chlorophenol red

Zero point one gram (0.1g) of chlorophenol red was dissolved in a 250 cm^3 flask containing 23.6 cm^3 of 0.01M sodium hydroxide (NaOH) which aids with the dissolution of chlorophenol red. The paper was soaked in this solution, drained and dried in an oven to achieve a yellow colour (Figure 3.2). The paper was then cut into small strips and stored in a desiccator with dry silica gel.

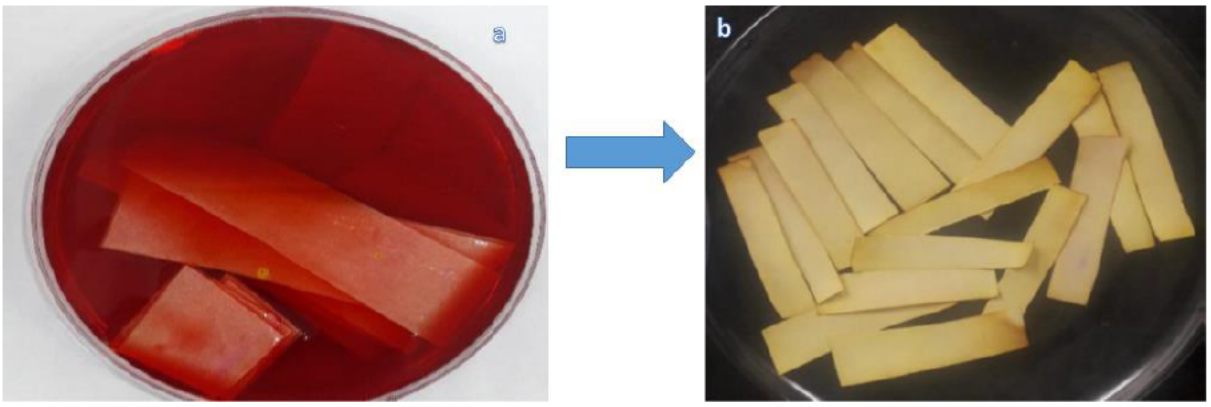

Figure 3. 2: Showing Chlorophenol (a) Soaked filter cholrophenol red (b) Oven dried test strip

3.2.2 Preparation of Cobalt (II) Chloride

For the Cobalt (II) Chloride, 5g hydrated cobalt (II) chloride was dissolved in 100cm^3. As shown in Figure 3.3, the fabricated papers were placed in the prepared solution and thereafter dry in an oven (set at no more than 100°C). After drying, the papers were stored in a desiccator with a dry silica gel to prevent the absorbance of moisture.

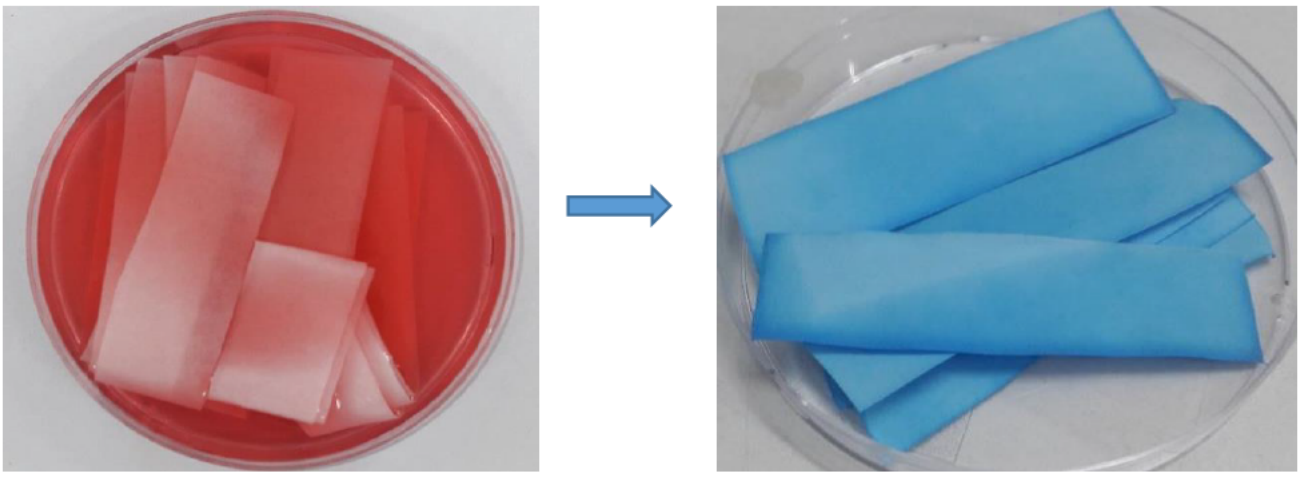

Figure 3. 3: Showing Cobalt (II) Chloride (a) Soaked filter cholrophenol red (b) Oven dried test strip

3.2.3. Scanning Electron Microscopy observation of the microfluidic paper (SEM)

Scanning electron microscope (Field Emission-Carl Zeiss) operating at controlled atmospheric conditions at 20 kV was used to examine the surface structure of the developed uPAD devices. Prior to SEM observation, the surface was coated with a thin, electric conductive gold film to prevent build-up of electrostatic charge.

3.4 Humidity test

Humidity test was conducted using EQ 072 and EQ 073 humidity devices. EQ 072 was used to test the humidity at 0:59 am and at a temperature of 22°C. The measured humidity was 68%. Cobalt (II) chloride changed colour back to pink at humidity above 55% whereas there was no colour change on chlorophenol red at above 55% humidity on the blank tests conducted (Figure 3.4).

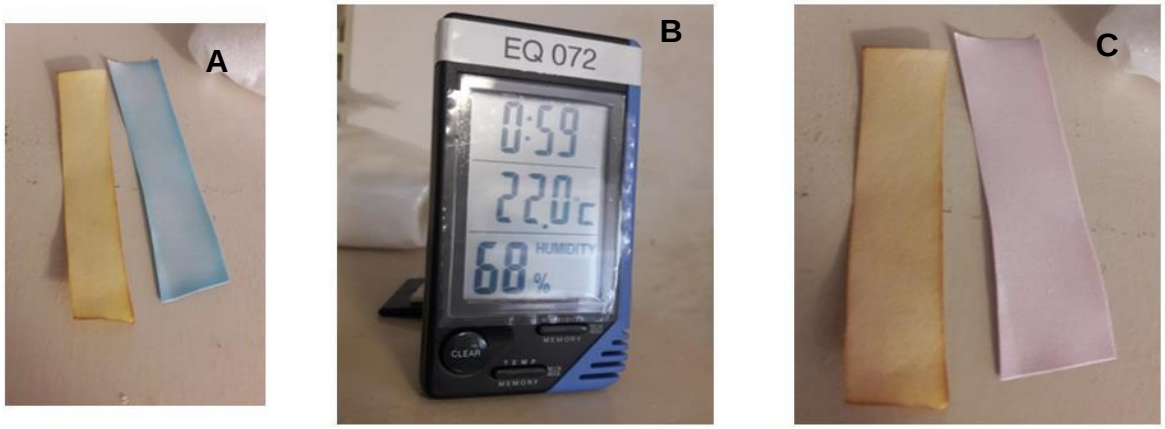

Figure 3. 4: Showing humidity test at 0:59 am and at a temperature of 22°C: (A) before test (B) EQ 072; (C) after test

EQ 073 was used to test humidity test at about 7:04 am at a temperature of 18.3 °C. The humidity was found to be 80%. Cobalt chloride strips after approximately 7

minutes of air exposure in an environment of humidity above 55% indicated a colour change back to pink, and no colour changed observed on chlorophenol red strips after approximately 60 minutes of air exposure at humidity above 55% (Figure 3.5).

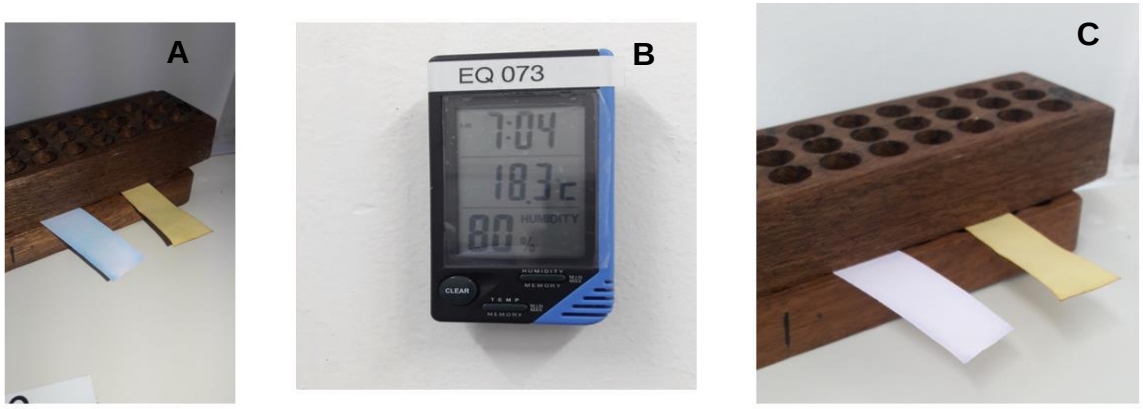

Figure 3. 5: Showing humidity test at 7:04 am and at a temperature of 18.3 °C: (A) before test (B) EQ 073; (C) after test

3.5 pH test on Chlorophenol red test strips

To determine the colour change at different pH, the Chlorophenol red test strips were treated with tap water of different pH levels. Chlorophenol red colour change varies with pH. It is more yellow in highly acidic (Figure 3.6 A) solutions and purple in highly basic solutions (Figure 3.6).

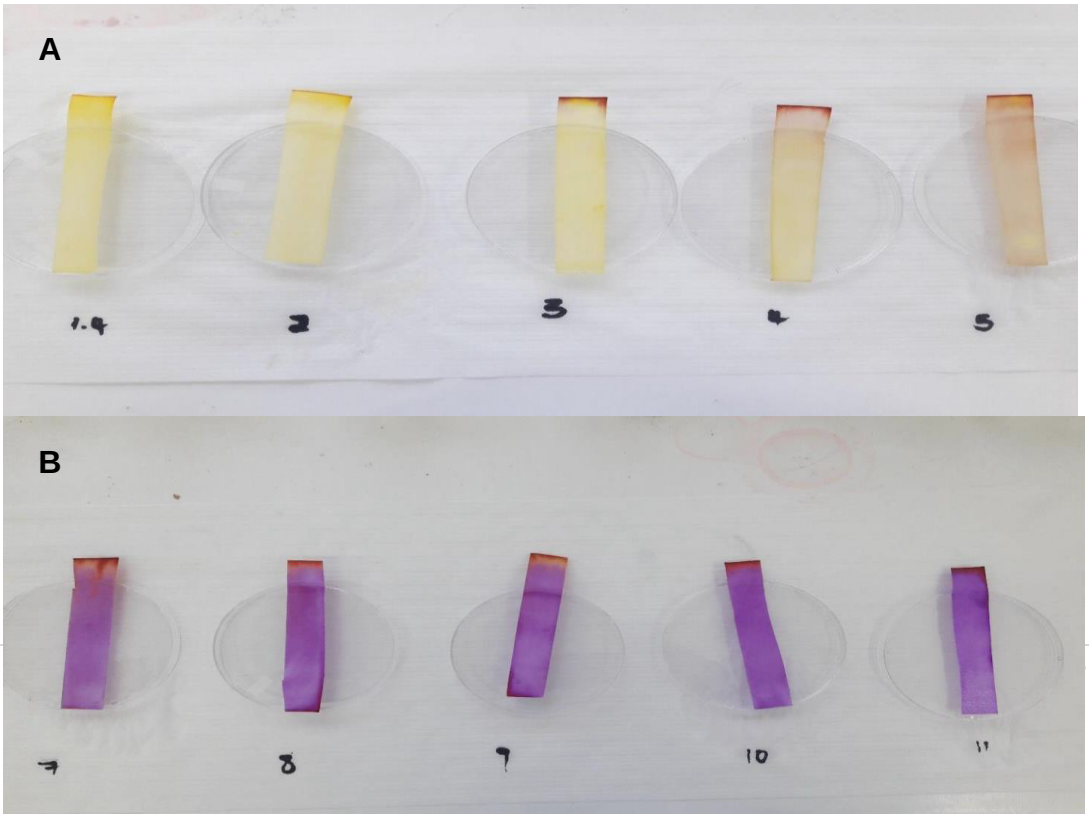

Figure 3. 6: Showing pH of test strips (A) acidic water; (B) basic water

3.5.1 Verification of pH using plastic cuvette

The pH of the colorimetric test strip was also verified using a cuvette (Figure 3.7). The colours in Figure 3.7(b) were obtained by buffering to obtain pH 1 to 10. The concentration of acetic acid and sodium hydroxide was 0.01M and was added into 200ml beaker in drops while using a stirring rod to get the homogenous mixture. Thereafter, the pH was then tested using the benchtop pH meter. Prepared mixtures were then poured into sample bottles and labelled pH 1-10 (Figure 3.7a). From the prepared mixture, about 4ml was transferred into clear cuvette and added a drop of Chlorophenol red, and colour change was observed as presented in Figure 3.7b. The drops (one drop) of prepared mixture were then introduced on the Chlorophenol red filter paper and colour change was observed (Figure 3.7c).

(a)

(b)

(c)

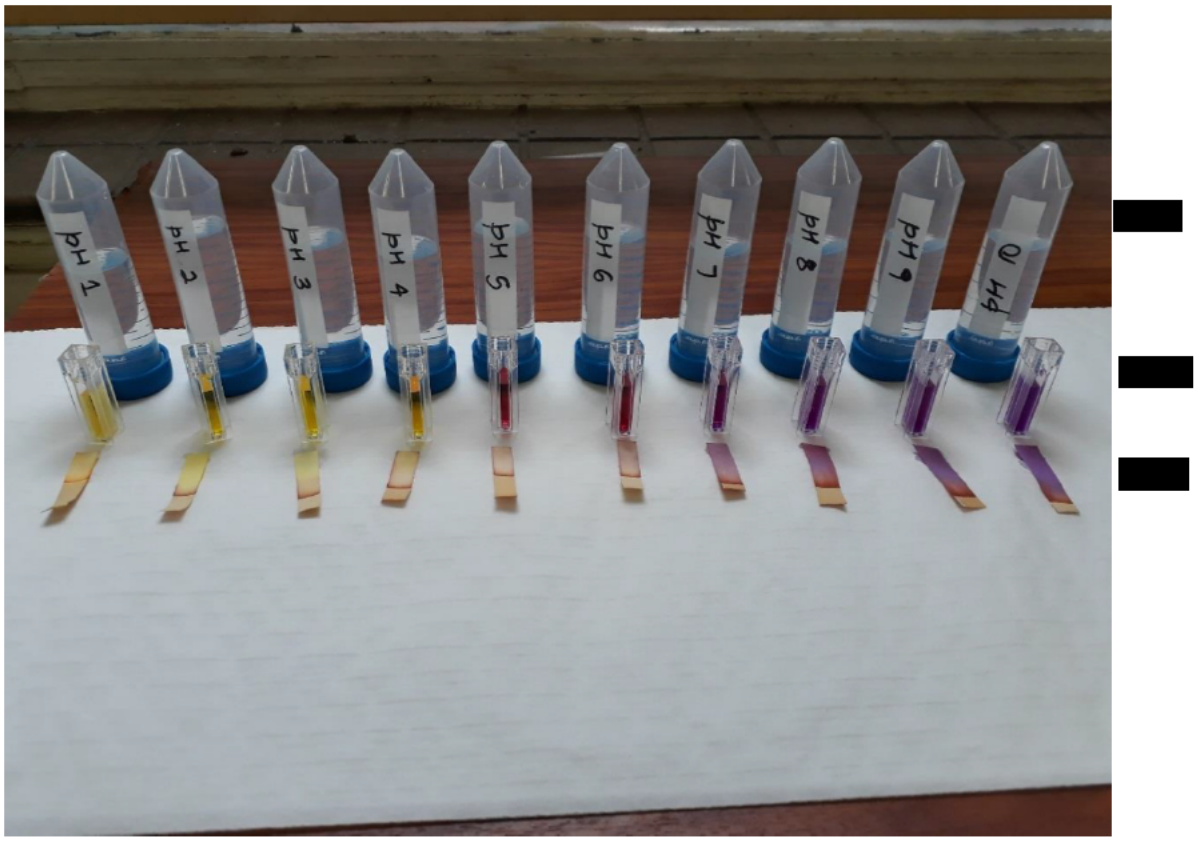

Figure 3. 7: Showing the verification of pH (a) prepared pH solution, (b) cuvette colorimtric devices (c) filter paper

3.5.2 Verification of pH using Lovibond colorimetric filter

CorelDraw home and student X7 was used for the design of Lovibond colour filter. The colour filter was printed on a plastic slide using a wax printer (ColorQube 8570DN, Xerox). The fabricated Lovibond colour filter was used to confirm the pH observed using both the cuvette and colorimetric filter paper. This was done to optimise the fabrication process. The complimentary reading for each colour was printed at angle of 90º of the complimentary colour (Figure 3.8).

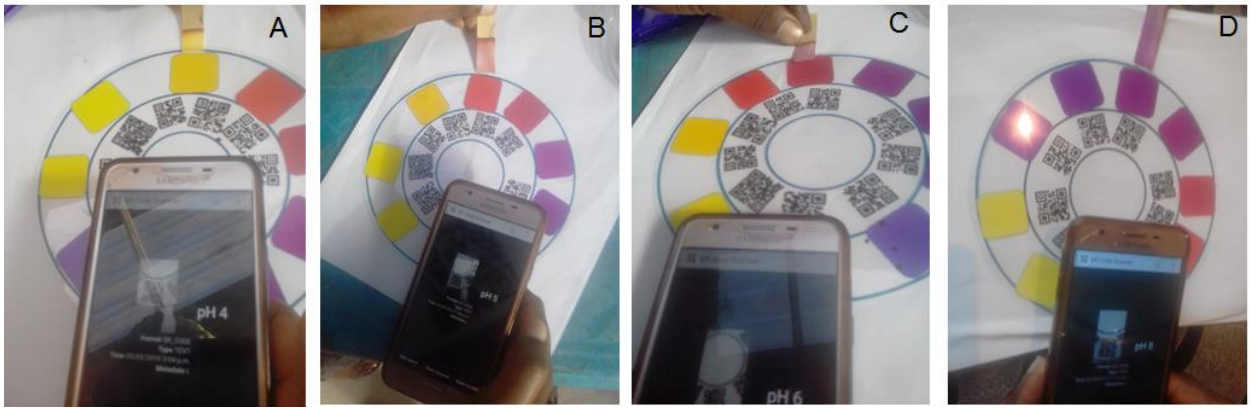

Figure 3. 8: Showing the pH reading using Lovibond filter (A) pH 4, (B) pH 5; (C) pH 6; and (D) pH 8

3.5.3 Validation of the colour change using UV Spectrophotometer

To help validate the colour change using UV Spectrophotometer, 10mL of tap water of different pH was mixed with 3mL (Table 3.1) as well of 3 drops (Table 3.2) of chlorophenol red indicator. This was left to stand for 10 min and then read. It was worth noting that the different pH of tap water were obtained by diluting the tap water with sodium hydroxide solution.

3.5.4 Optical Electron Microscopic Observation of colour

The pH colour change was further validated using optical electron microscope (model Bx45; Olympus Corp). A drop of the prepared pH 1-10 was placed on the colorimetric filter paper and the colour change captured.

3.6 Location

Although South Africa has 9 provinces, the study location was, however, limited to KwaZulu-Natal and Gauteng (Figure 3.9).

Figure 3. 9: Map of study location

3.7 Google analytics

Google analytics account was created using Google whereby simple steps were followed to sign up. The website URL for this study is (https://zodidi68.wixsite.com/website)where one can find more information about the results obtained. Quick Response (QR) code was downloaded using the smartphone which enables the tracking and to obtain the location from which a leakage was detected. The website is tracked by google analytics on how many leaks reported (real-time view) and where exactly those leaks are situated. GPS locations can be viewed by country, province, city etc. Other trackable QR barcode were created using online tool at https://phumlani.grd.by/user/help/gps#activation

3.8 Leak detection test

The Fabricated chlorophenol red test strip was taken and wrapped around water pipes on various places to detect leakages (Figure 3.10 and 3.11). The strip turned purple/violet immediately where water leaks were observed and did not change on dry pipes. The colour change was captured with a smartphone, thereafter, transferred to a computer for colour measurements. Image J software was used to measure the intensity of the colour formation in the detection zones. The RBG (red, green, blue) colour intensity profile plot was obtained for a chord passing through the centre of each detection zone.

Figure 3. 10: Showing (A) detection of leaking pipe; (B) Leak detection using colour grab App

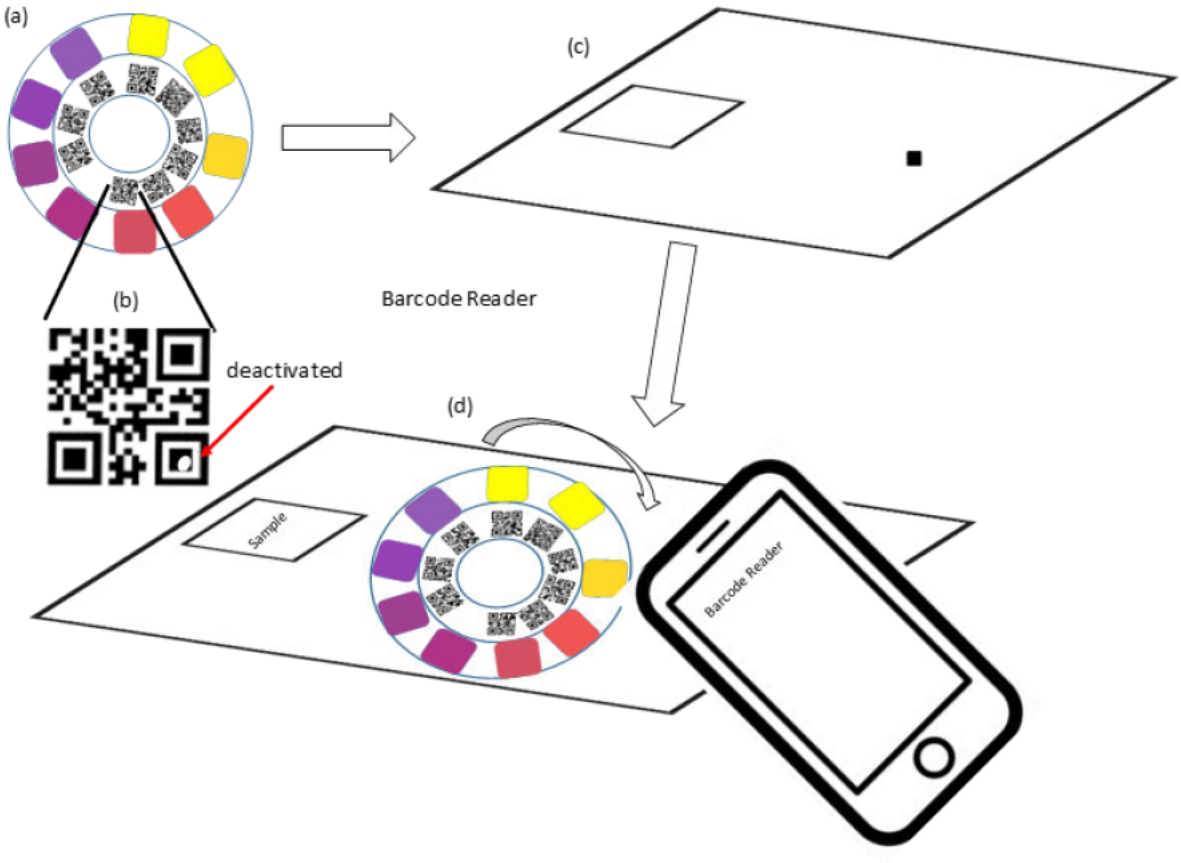

Figure 3. 11: Schematic illustration of trackable analytical real time water detection device

CHAPTER FOUR

RESULTS AND DISCUSSION

The results and discussion of the study are presented in this chapter. The data collected were analysed in relation to the research objectives as outlined in Chapter One, that is: the design and fabrication of microfluidic device using chromatographic paper to detect water leaks; optimised and standardise the pH, humidity, and indicators for the paper based device, and the development of a real-time Google analytical device to tract water leaks. The results are presented using virtual images and colour changes. This chapter concludes with a summary of the data that was analysed

4.1 Scanning Electron Microscopic Observation of the device

The microstructure and elemental composition of the microfluidic paper before and after chlorophenol red application are given Figure 4.1. As shown in Figure A1 and A2, the porous structure of the paper are visibly evident. The porous structure of the paper is in agreement with Costa *et al*. (2014) that chromatography paper has a high porosity (~68%) with a corresponding higher pore diameter (100 µm). The EDX images, by contrast, revealed differences in the elemental composition of the paper before and after indicator application. For example, the EDX spectrum before indicator application (B1) revealed the present of carbon (C), oxygen (O) and Sodium (Na). The presence of these elements may be attributed to the composition of the chromatography paper which is primarily cellulose. Costa *et al*. (2014) reported that chromatography paper are manufactured from high quality cotton liners that have been treated to achieve a high cellulose content (>98%). On the contrary, the presence of chlorine was evident in the EDX spectrum after indicator application (B2), which may be attributed to the chlorophenol red.

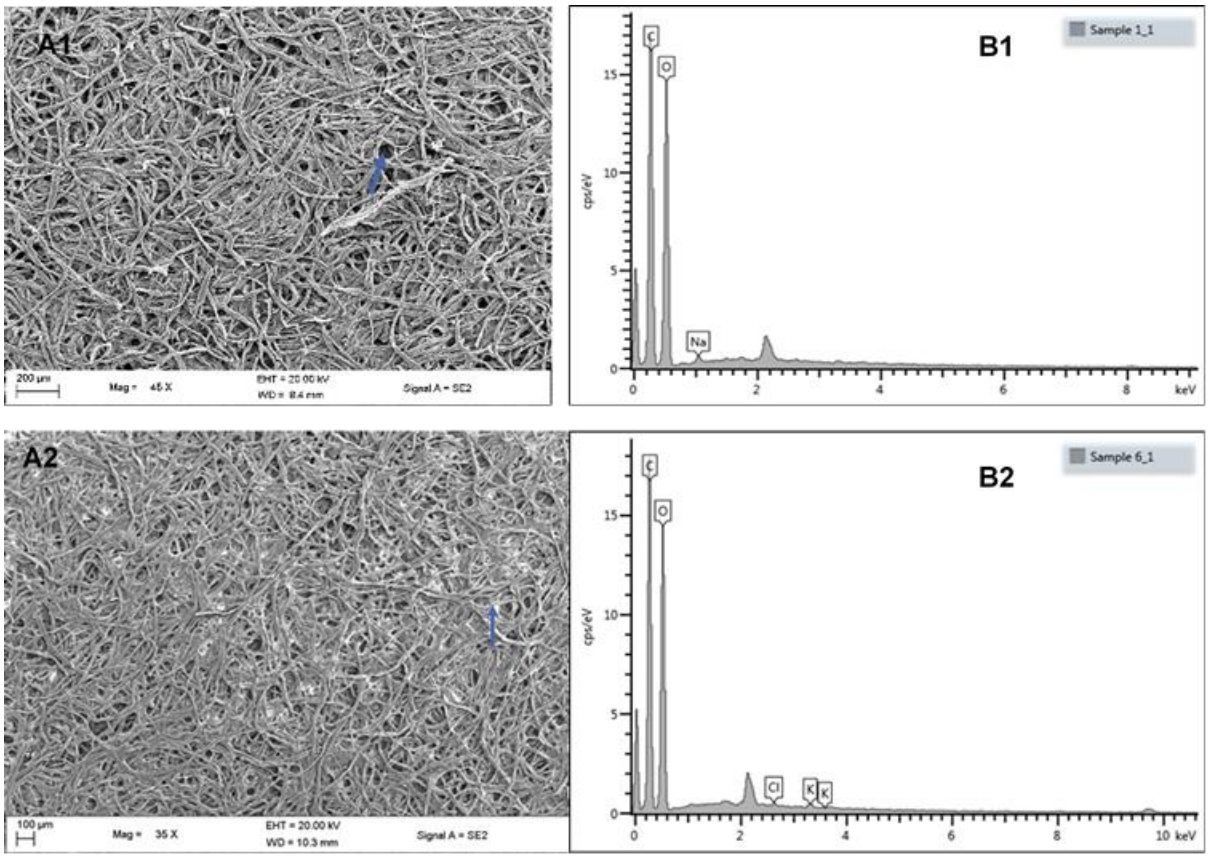

Figure 4. 1: Showing (A) SEM images of chromatography paper (B) EDX elemental composition (1-before; 2-after indicator application)

4.2 Stability of the fabricated microfluidic paper

As described in Chapter three, Section 3.4, the humidity test reveals that Chlorophenol red was more stable (Figure 3.5) than cobalt chloride (Figure 3.6) when exposed to moisture. From a chemistry perspective, and although cobalt chloride compound have been the chemical of choice for detecting water leaks due to its ability to change from blue to pink when it comes in contact with water (American Chemistry Council 2006), it is however, not suitable for use in this study because of the high humid nature of the study area. More so, cobalt chloride changes colour rapidly in response to humidity above 55%. This characteristics may give a false results in area of high humidity.

Of importance, the irreversible colour change observe for Chlorophenol test when exposed at a humidity of above 55% suggest that it is more suitable for used in this study since it offers better stability in high humidity. This is in agreement with Indigo

Instrument (2019) that chlorophenol red gives a more permanent and very distinctive water indication. Hence it is sufficient to assume that Chlorophenol prepared test strips will not interfere with the leak detection test. The colour variation of chlorophenol was studied using CIELab as shown in Figure 4.2. It can be noted in Figure 4.2 (a,b) that there was an increase of blue colour as well as the z values in the XYZ graph as the pH was increased which was in agreement with colour obtained after reaching pH12 which was purple. The pH variation is very vital since the pH of water may change depending on the source. However, the pH of drinkable water is 7 thus for all leaking pipes with drinking water would give pH 7. More so, it is again clearly visible that data obtained from CIEy in Figure 4.2 (c) support this observation with plotted data mainly occupying the purple region of the horse shape.

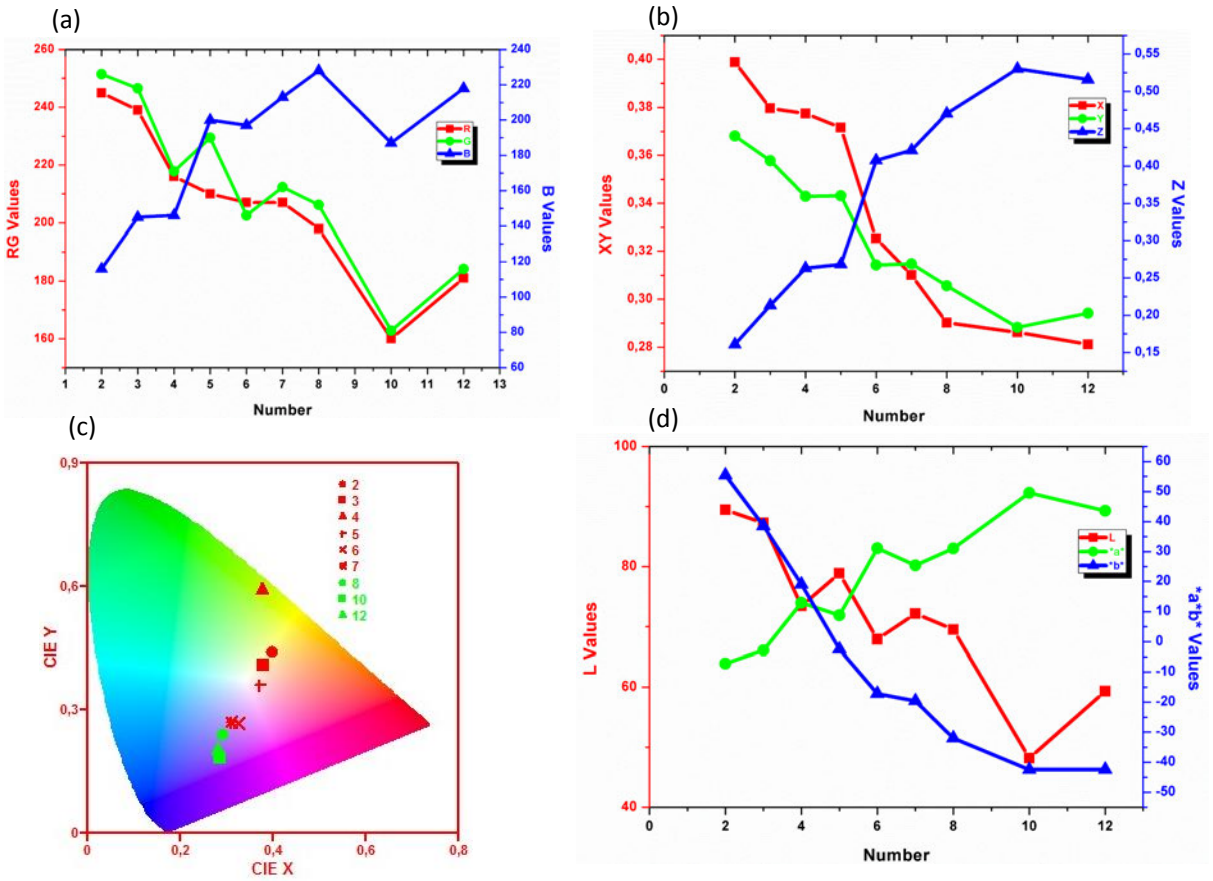

Figure 4. 2: CIELab colour scheme of cholorophenol red strip at difference pH, (a) RBG curve (b) XYZ colourrimetri plot, (c) horse shoe shaped CIElab color scheme and (d) plot of the Lab values.

Further to understanding colours using CIELab as described above, it was very important to look at colour variation using ΔE as shown in Figure 4.3. The result in Figure 4.3 (a) shown that there was a huge change in the colour as the pH was increased which supported CIELab colours. This variation was observed with the plot of colour differences (ΔE) increasing from 0 to 120 as the pH was increased as well. The R/G ratio was plotted in figure 4.3(b,c and d) which agreed very well with the RBG curve as discussed above where the blue colour increased for basic solutions.

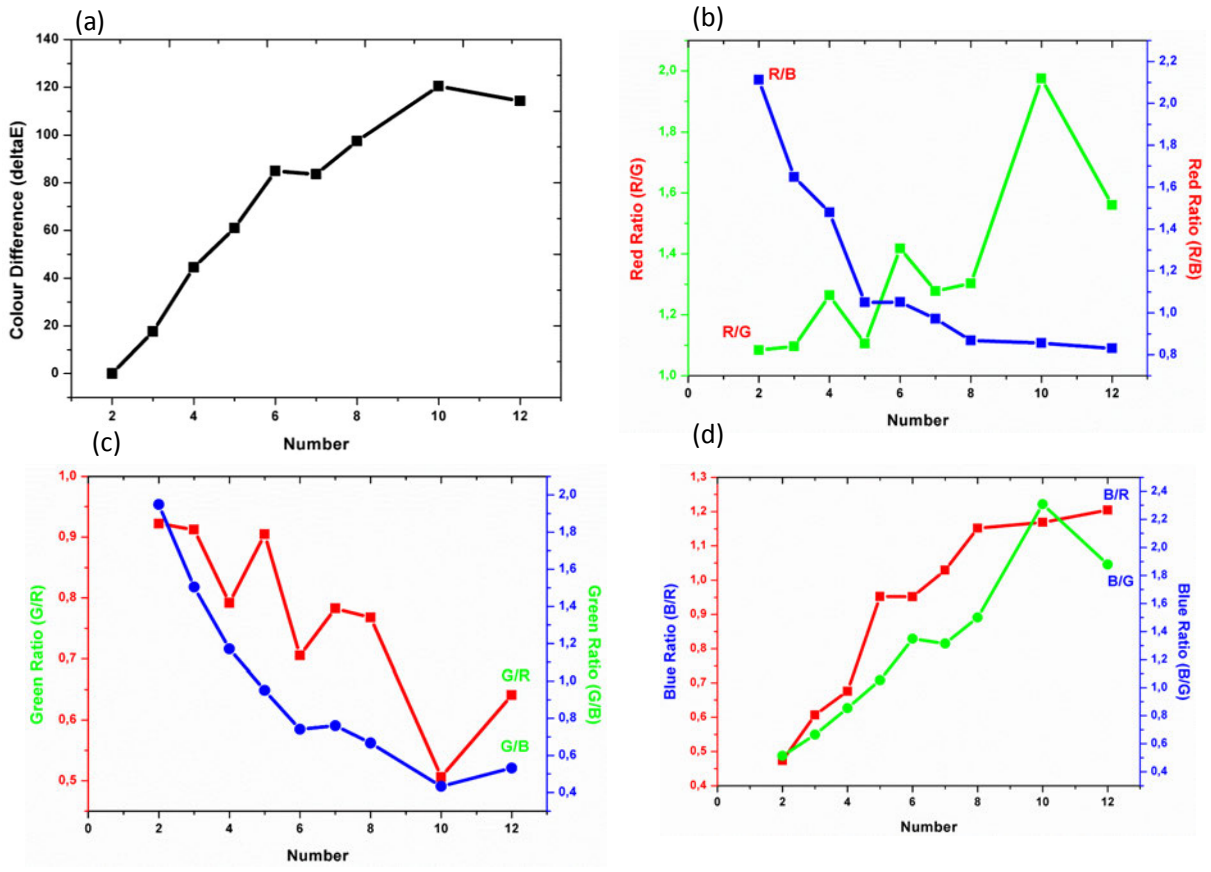

Figure 4. 3: Plot of (a) colour differences (b,c and d) plot of the ratio of red, green and blue colours from acidic to basic solution.

4.2 Colour Absorbance versus pH

The colour accuracy of the images captured for the μPADs at different pH in Figure 4.4 were established by measuring the RGB (red, green and blue) values and using CIELab (Commission Internationale de l'Eclairage) colour space determination. According to Liu and Yang (2013), the RGB colour model is premised on the science that the human eye perceives light and translate same into brain waves. Accordingly, and based on the aforesaid principle, the colorimetric image of water

samples at different pH were analysed for their RGB values using Image J Software. The obtained RGB colour histograms showing the pixels and the RGB values at different pH are given in Figure 4.4. It was observed that at highly acidic solutions the graph is even and when approaching pH 4 the graphs starts rising until about pH 10 and then starts levelling for most basic pH solutions. These trend could be attributed to the fact that chlorophenol red colour change remain unchanged at a pH of water below 5.5.

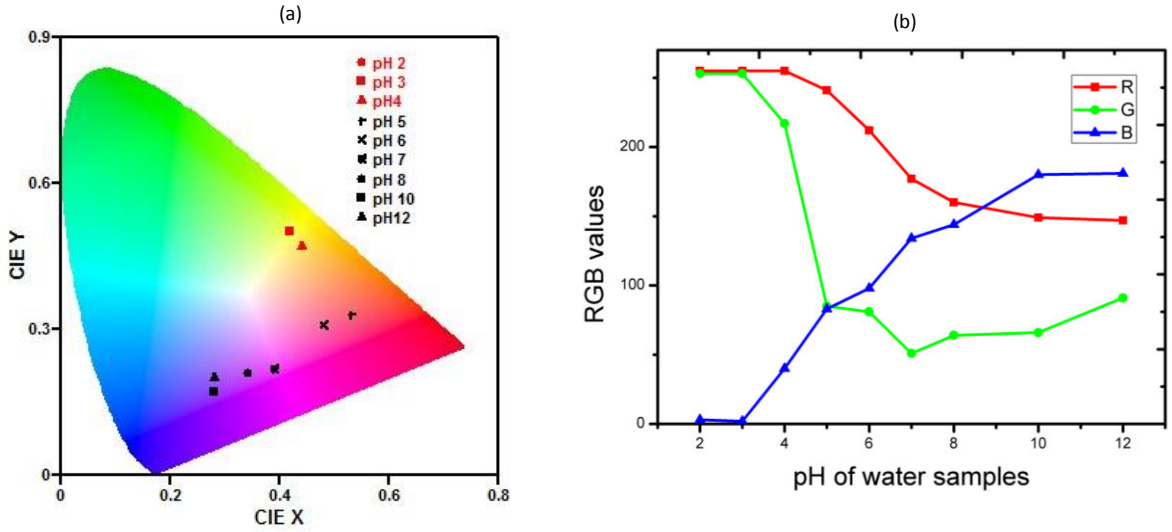

Figure 4. 4: Graph showing of colour change (a) CIEb lab; and (b) RGB values of water samples there were validated using spectrophotometric analysis.

For the above reason, and although the chlorophenol red colour change varies with pH, it is more yellow in highly acidic solutions and more purple in highly basic solutions. With this variation the researcher validate the colour change by reading the solutions on different pH levels with three drops of the indicator at 572 nm wavelength (Table 4.1). It was observed that at highly acidic solutions the graph was even and when approaching pH 4 the graphs starts rising until about pH 10 and then starts levelling for most basic pH solutions (Figure 4.5). This made it difficult to tell the difference in colour intensities for pH 1 and 2. The result were further analysed using ImageJ, which showed a change in intensity with changing the pH of water as shown in Figure 4.5 below.

Table 4. 1: Readings of pH with 3drops indicator

pH	Absorbance at 572nm
2	0.001
4	0.008
6	0.484
8	0.621
10	0.651
12	0.656

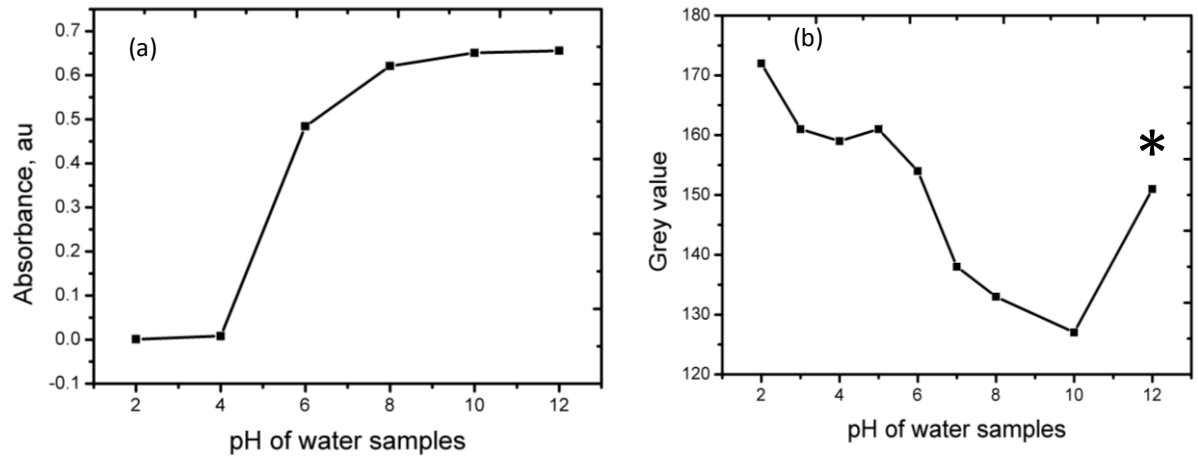

Figure 4. 5: graph of absorbance at 572nm Vs pH

4.2.1 Image validation of the colour change and pH using Optical microscope

Apart from the spectroscopy validation using the absorbance value, the colour change was also validated using optical microscope observation (See Figure A3 c). The optical microscope image provides a visible evidence in the colour change comparative with the RGB (Figure A3 b) and curvette (Figure A3 a). This can also be further supported by the CIElab colour chroma in Figure A4 (b).

4.3 Leak detection test

Having validated the test trips, the fabricated chlorophenol red test strip was then wrapped around the water pipes on various places to detect leakages. The strip turned purple/violet immediately where water leaks were observed and did not change on dry pipes (Figure 4.6). The system can be made to be a network of plumbers and or municipal personnel that attends to the leaks. Chromatographic paper is an inexpensive, biodegradable, and combustible material; porous structure

of paper makes it ideal for lateral flow assays and chromatography applications; paper devices can be easily used successful for detection of water with the chlorophenol strips, the strips are then tracked using google analytics for each scan made (Figure 4.7). Scanning the QR codes takes the smartphone user to a website that has information on the chlorophenol red test stripes and has contact details. Whilst on the website it is possible to track the user's location using GPS making it easier to respond on time on detected water leaks (Table 4.2).

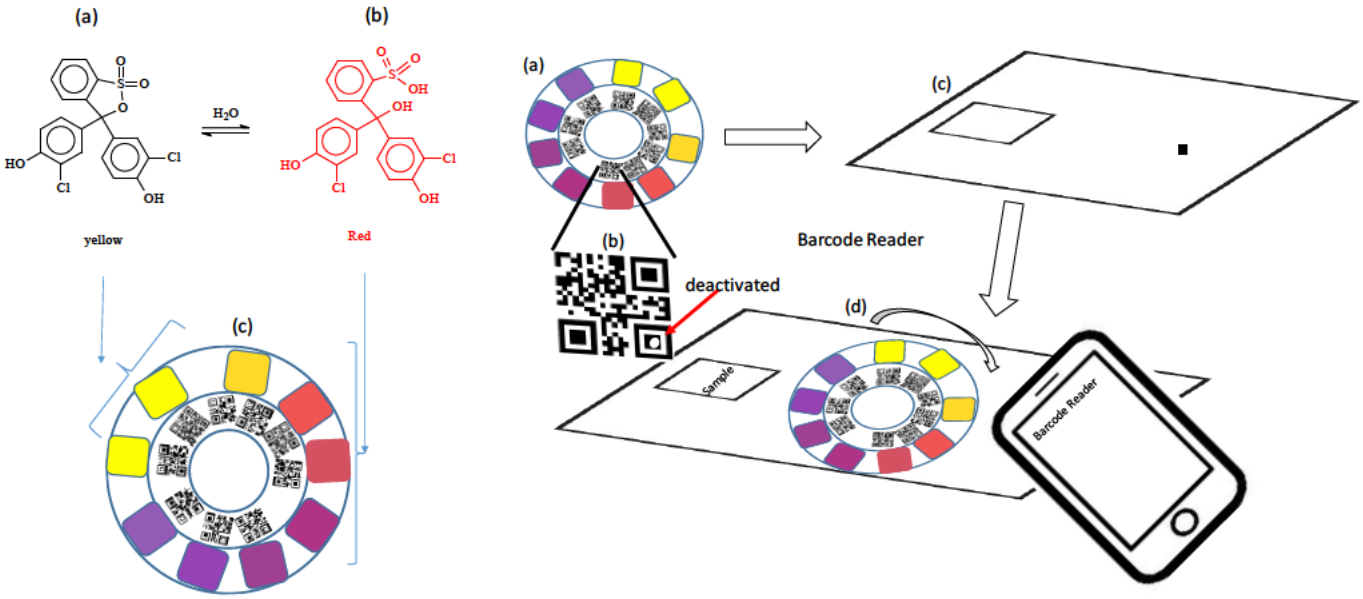

Figure 4. 6: Schematic illustration of traceable analytical real time water detection device

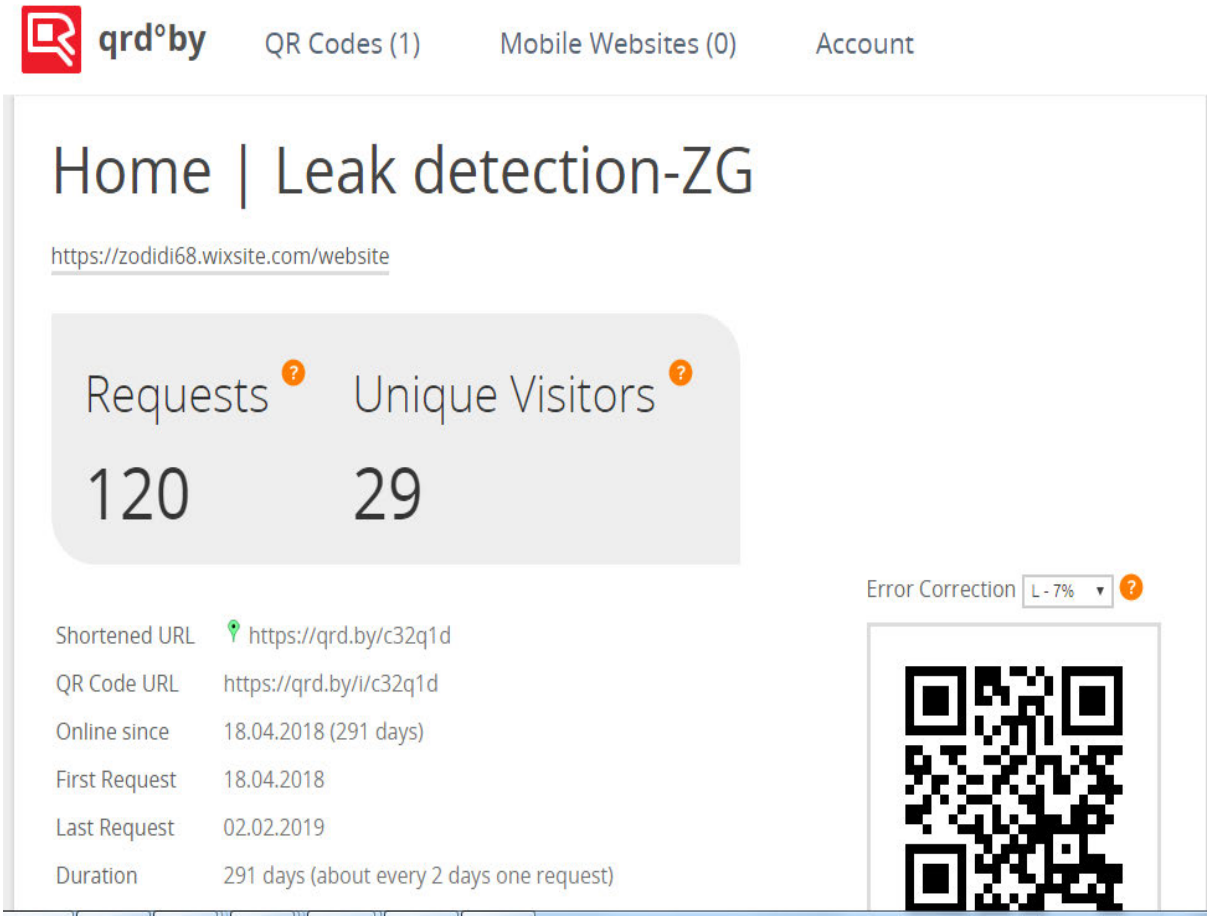

Figure 4. 7: Shows the number of request made by people to detect water leaks

The colour change was captured with a smartphone, thereafter, transferred to a computer for colour measurements. ImageJ software was used to measure the intensity of the colour formation in the detection zones. The RBG (red, green, blue) colour intensity profile plot was obtained for a chord passing through the centre of each detection zone. Figure 4.8 (a) shows plots of grayscale and absorbance against the pH of water analysis values. A significant decrease was observed from the plot of grayscale against pH between 2-10, whereas, a significant increase was noticed in the plot of absorbance against pH values of water analysis in the range of 2-12 indicating that the absorbance is directly proportional to pH. The red and the green coordinates decreased rapidly while a rapid increase was noted in the blue

coordinates as the pH values increased in Figure 4.8 (b) representing the RGB curves.

The RGB colour coordinates for each pH value were converted to L, a* and b* values using website conversions (http://colormine.org/convert/rgb-to-hunterlab) (McLaren 1976; Yusufu and Mills 2018). The L and the b* curves decreased rapidly as the pH increased Figure 4.8 (c) indicating that as the pH increased the water became darker. The gradual increase in pH 5 in a* curve suggested that water was red and after that it started to drop leaning towards the green region. Colour difference, chroma and hue angle were calculated using equation (1), (2) and (3), respectively. The L_0, a_0* and b_0* for the ΔE were the colour produced at initial pH 2. Colour difference curve in Figure 4.8 (d) increased monotonously with increasing pH value of water analysis. Chroma decreased gradually with the increase in pH indicating that the water was dull. A steep rise in hue angle was obtained between pH 4-5.

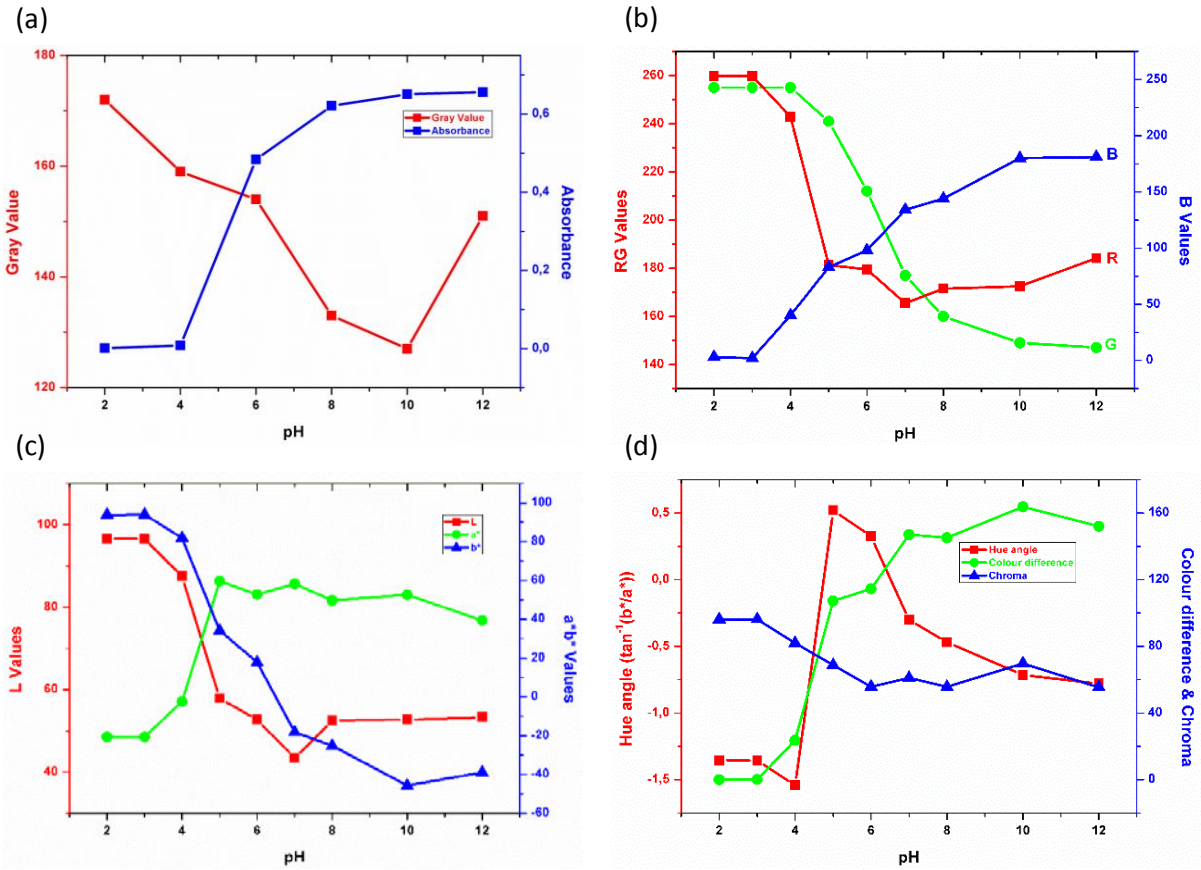

Figure 4. 8: (a) Graph of absorbance at 572 nm and grayscale value against pH, (b) Plots of (a) RGB colour coordnates against pH value, (c) La*b* values against pH and (d) Plots of ΔE, hue and chroma vs pH

4.3.1 Real-time measurement

Table 4.2 below show the real-time users from the website and their locations. This proved that the QR code scanned was conveying data to google analytics. The data was catergorised based on trackable and untrackable leaks as follows:

- Leaks detected but not trackable
- Leaks detected and trackable

In table 4.2, it was observed that the information on the device used during scanning was captured in the data received from Google analytics, other vital information and GPS coordinate were also captured in the Google analytics data. More data of this nature are provided in Table A1in the appendix section. From **Table A1, 2 and 3**, it could be noted that map preview of all tested sample can be presented using maps, which were easily zoomed to preview street, and other information required to mitigate water loses because of leaks.

Table 4. 2: Schematic illustration of Google analytics which can tell real-time users from the website and their locations[1].

Date	Time	Type of Smart phone	Country and Province
18.04.2018	15:23 PM	Samsung SM-G570F	South Africa
		Chrome Mobile 64 (Android 6.0.1)	KwaZulu-Natal, Durban
		Lng/Lat: 30.8707, -29.8594 (accuracy: 28 meters)	
02.05.2018	15:41	Samsung SM-G570F	South Africa
		Chrome Mobile 64 (Android 6.0.1)	KwaZulu-Natal, Durban
		Lng/Lat: 30.8707, -29.8594 (accuracy: 24 meters)	
04.05.2018	23:44	Samsung SM-G570F	

[1] More tracked data are given in the appendix section in **Table A1**

			South Africa
		Chrome Mobile 64 (Android 6.0.1)	KwaZulu-Natal, Ballito
		Lng/Lat: 30.891, -29.8723 (accuracy: 12 meters)	
05.05.2018	12:34 PM	Samsung SM-G570F	South Africa
		Chrome Mobile 64 (Android 6.0.1)	KwaZulu-Natal, Durban
		Lng/Lat: 31.0098, -29.8503 (accuracy: 17 meters)	
05.05.2018	12:42	Samsung SM-G570F	South Africa
		Chrome Mobile 64 (Android 6.0.1)	KwaZulu-Natal, Durban
		Lng/Lat: 31.0098, -29.8503 (accuracy: 22 meters)	
05.05.2018	15:46	Samsung SM-G570F	South Africa
		Chrome Mobile 64 (Android 6.0.1)	KwaZulu-Natal, Durban
		Lng/Lat: 31.0061, -29.8494 (accuracy: 9 meters)	
12.05.2018	13:01	Samsung SM-G570F	South Africa
		Chrome Mobile 64 (Android 6.0.1)	Western Cape, Cape Town

		Position could not be retrieved	
12.05.2018	02:31 PM	Samsung SM-T116	South Africa
		Chrome 66 (Android 4.4.4)	KwaZulu-Natal, Durban
		Lng/Lat: 31.0097, -29.8502 (accuracy: 30 meters	
12.05.2018	13:53	Samsung SM-G570F	South Africa
		Chrome Mobile 64 (Android 6.0.1)	Western Cape, Cape Town
		Position could not be retrieved	
12.05.2018	14:00	Samsung SM-G570F	South Africa
		Chrome Mobile 64 (Android 6.0.1)	Western Cape, Cape Town
		Position could not be retrieved	
12.05.2018	14:03	Samsung SM-G570F	South Africa
		Chrome Mobile 64 (Android 6.0.1)	Western Cape, Cape Town
		Position could not be retrieved	
12.05.2018	14:24	Samsung SM-G570F	South Africa
		Chrome Mobile 64	Western Cape, Cape

		(Android 6.0.1)	Town
		Position could not be retrieved	
12.05.2018	14:31	Samsung SM-T116	South Africa
		Chrome 66 (Android 4.4.4)	KwaZulu-Natal, Durban
		Lng/Lat: 31.0097, -29.8502 (accuracy: 26 meters)	
15.09.2018	19:45	Samsung SM-G570F	South Africa
		Chrome Mobile 68 (Android 6.0.1)	KwaZulu-Natal, Durban
		Lng/Lat: 30.8895, -29.875 (accuracy: 1600 meters)	
15.09.2018	19:46	Samsung SM-G570F	South Africa
		Chrome Mobile 68 (Android 6.0.1)	KwaZulu-Natal, Durban
		Lng/Lat: 30.8895, -29.875 (accuracy: 1600 meters)	
06.10.2018	06:04	Samsung SM-G570F	South Africa
		Chrome Mobile 69 (Android 6.0.1)	KwaZulu-Natal, Durban
		Lng/Lat: 30.8906, -29.8727 (accuracy: 1200 meters)	

06.10.2018	06:35	Samsung SM-G570F	South Africa
		Chrome Mobile 69 (Android 6.0.1)	KwaZulu-Natal, Durban
		Lng/Lat: 30.8906, -29.8727 (accuracy: 12 meters)	
06.10.2018	06:36	Samsung SM-G570F	South Africa
		Chrome Mobile 69 (Android 6.0.1)	KwaZulu-Natal, Durban
		Lng/Lat: 30.8906, -29.8727 (accuracy: 1200 meters)	
13.10.2018	15:06	Samsung SM-G570F	South Africa
		Chrome Mobile 69 (Android 6.0.1)	KwaZulu-Natal, Durban
		Lng/Lat: 31.0065, -29.8493 (accuracy: 900 meters)	
13.10.2018	15:07	Samsung SM-G570F	South Africa
		Chrome Mobile 69 (Android 6.0.1)	KwaZulu-Natal, Durban
		Lng/Lat: 31.0098, -29.8502 (accuracy: 25 meters)	
13.10.2018	15:08	Samsung SM-G570F	South Africa
		Chrome Mobile 69 (Android 6.0.1)	KwaZulu-Natal, Durban

		Lng/Lat: 31.0097, -29.8503 (accuracy: 18 meters)	
13.10.2018	15:10	Samsung SM-G570F	South Africa
		Chrome Mobile 69 (Android 6.0.1)	KwaZulu-Natal, Durban
		Lng/Lat: 31.0097, -29.8503 (accuracy: 18 meters)	
18.10.2018	10:00	Apple iPhone	South Africa
		Mobile Safari (iOS 12.0)	Gauteng, Johannesburg
		Position could not be retrieved	
18.10.2018	10:10	Apple iPhone	South Africa
		Mobile Safari (iOS 12.0)	Gauteng, Johannesburg
		Position could not be retrieved	
18.10.2018	10:45	Apple iPhone	South Africa
		Mobile Safari (iOS 12.0)	Gauteng, Johannesburg
		Lng/Lat: 31.0097, -29.8503 (accuracy: 46 meters)	

In summary, the use of a simple pH measurement in the microfluidic device in the early detection of water leakages was demonstrated. A colorimetric method based on the RGB colour coordinates, CIELa*b* colour difference (ΔE), hue and chroma was successfully optimised. Multiple colour changes due to the chlorophenol red pH indicator was suitable for a colorimetric pH measurement based on the use of ΔE. The combination of the μPADs and image analysis facilitated quantitative analysis for multiple colour changes and confirmed high assay reproducibility. The optimised paper-based analytical method will accelerate applications to point of care testing and in resource limited settings.

4.4 Future works

The pattern in figure 1 (a) will first be designed using appropriate software. The wax printer will then be used to print out the pattern on the appropriate paper. Hydrophobic barrier patterning is a key process to guide liquid to the desired path in paper-based analytical devices. Blue coballt chloride and Chlorophenol red will be immobilized in wells (iv) and (v). Upon, the exposure of well (i) in water, water be driven by capillary action while the hydrophobic barrier will direct the flow toward the immobilized indicator.

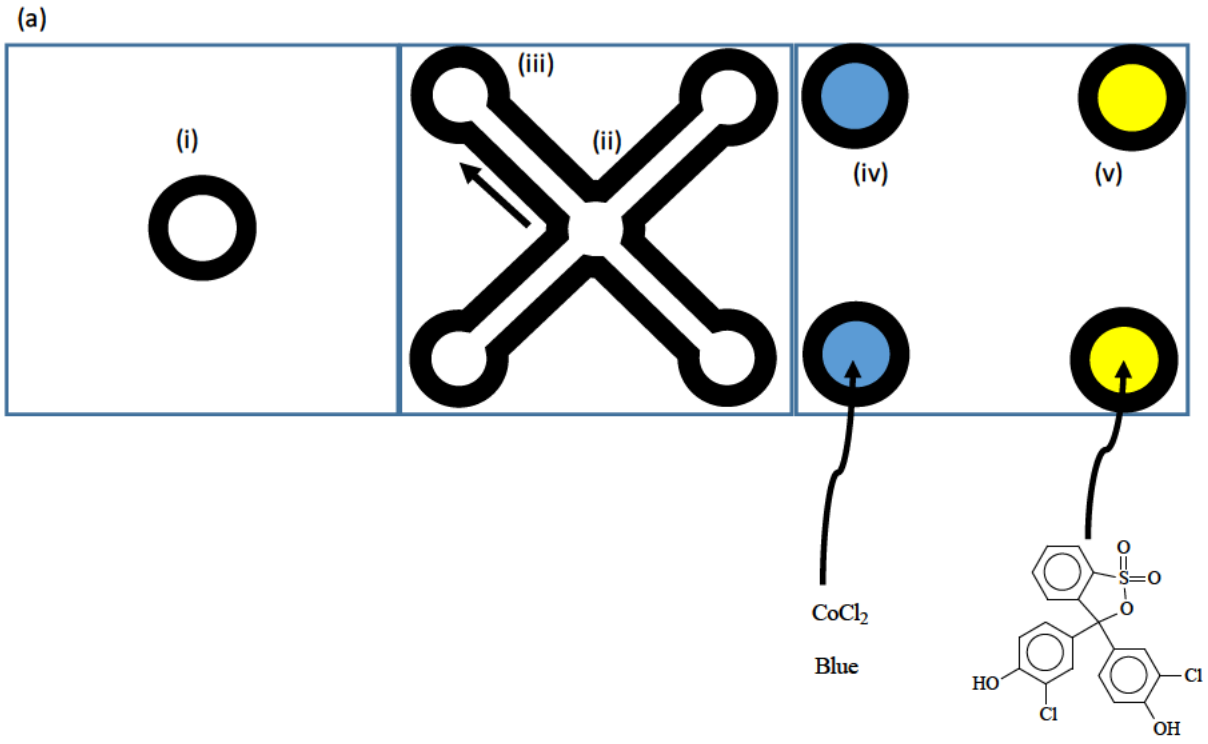

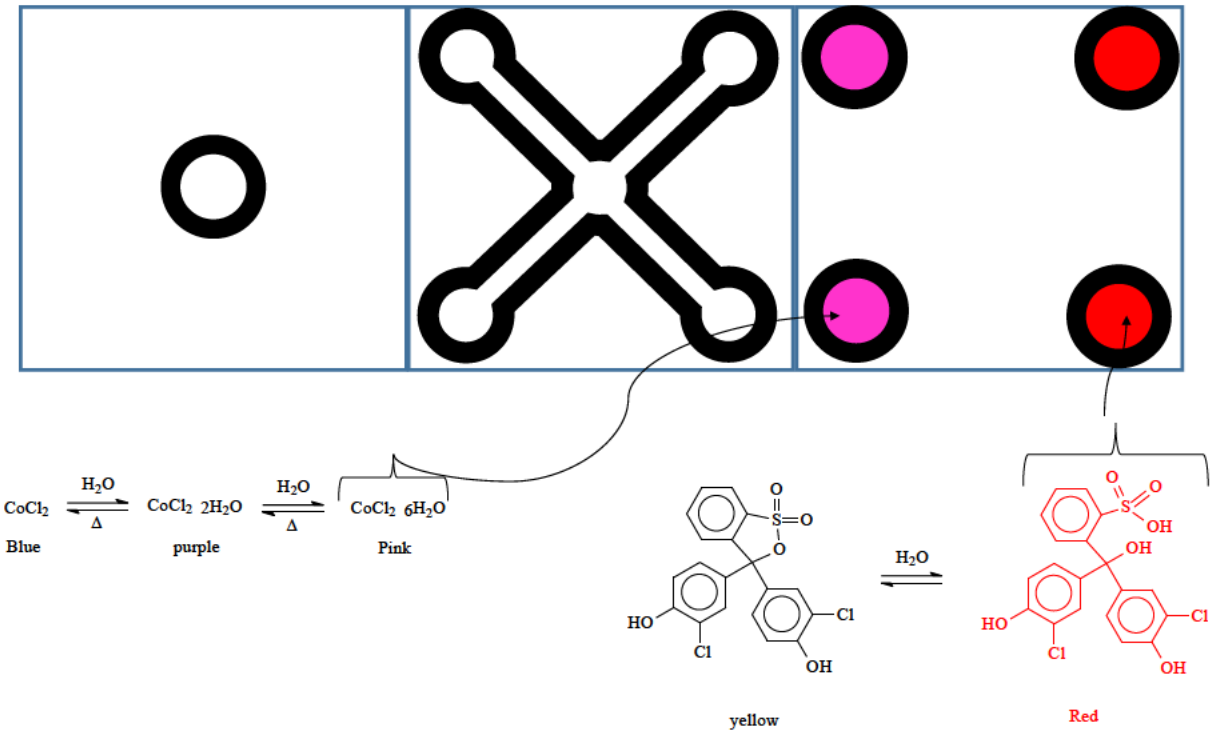

(b)

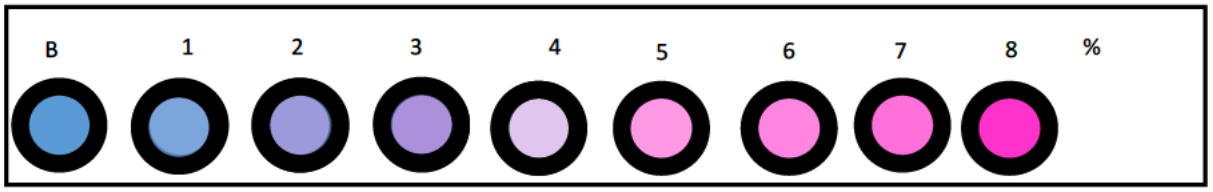

Figure 4. 9: Proposed design of michrofluidic strips for testing water leaks, where, (a) foldable paper chromatographic strips for testing fabricated with both Cobalt Chlorider and Chlorophenol Red, (b) proposed colour disk showing the change in colour of cobalt chloride by varying the concentration of water in %.

Chapter Five

CONCLUSION AND RECOMMENDATION

Given the concern of climate change and its long term consequence of water sustainability and availability, water leaks present a potent economic and health implications. As such, immediate identification and reporting of household leaks is the surest way of saving water. The focus of this study was to fabricate a trackable microfluidic device to detect water leaks. A quantitative research approach and an experimental research design was adopted. This chapter concludes by drawing on the objectives of the study to provide recommendations as well as proposed directions for future research.

5.1 Revisiting the research objectives

Objective One:

1.4.1.1 Design and fabrication of microfluidic device using chromographic paper to detect water leaks

The findings of this study have explicitly detailed the fabrication of a potable paper-based microfluidic device using chromographic paper and inkjet-printing technology. The developed device was successfully used to detect water leaks in a selected household based on colour change.

Objective Two:

1.4.1.2 Optimised and standardise the time, concentration and the volume the indicator.

In terms of ideal indicator, the results obtained indicate chlorophenol red offer more colour stability in a humid environment when compared to the cobalt chloride. It was observe that colour of the paper strips doped with cobalt chloride showed a reversible colour change in humidity above 55% while chlorophenol red remains stable. Three drops of Chlorophenol red was found to cause a colour change. Equally, the findings suggest that the paper strip colour change was more yellowish in acidic water and purple in highly basic solutions.

Objective Three:

1.4.1.3 The development of a real-time Google analytical device to track water leaks.

The study evidently demonstrates that the paper strip can provide a real-time of the leak location, and province using Google analytics. The result revealed that the QR code attached to the strips can easily be scan with a smartphone which directs the user to the website created for the purpose of the study (**https://zodidi68.wixsite.com/website**). Here, one can easily find more information about the results obtained.

5.2 Recommendations

Given the effectiveness of the fabricated device, the following recommendations are proposed:

- Chlorophenol red is recommended as the indicator of choice in a highly humid environment such as South Africa.
- It is recommended that future research be carried out in order provinces in South Africa and a larger household. This will help provide further support for the test strips in detecting water leaks.

In summary, this study has exhaustively demonstrates the use of paper-based microfluidic device. The fabricated µPADs which is yellow in colour when dry (due to the chlorophenol red indicator) is wrapped around the pipe suspected to have a leak. A colour change from yellow to violet/purple is observed instantly when there is a water leak. The website is tracked by google analytics on how many leaks reported (real-time view) and where exactly those leaks are situated. GPS locations can be viewed by country, province, city etc. This helps with timeous response to a leakage thus decrease the loss of water.

References

American Chemistry Council. 2006. *Cobalt Chloride: Colorful Moisture DetectorCobalt Chloride: Colorful Moisture Detector*. Available: https://chlorine.americanchemistry.com/Science-Center/Chlorine-Compound-of-the-Month-Library/Cobalt-Chloride-Colorful-Moisture-Detector/ (Accessed

Ballerini, D. R., Li, X. and Shen, W. 2012. Patterned paper and alternative materials as substrates for low-cost microfluidic diagnostics. *Microfluidics and nanofluidics*, 13 (5): 769-787.

Bertran, J. L. 2018. Examining Environmental Hazards in Rental Homes and Habitability Laws in Clark County, Nevada.

Bhakta, S. A., Borba, R., Taba Jr, M., Garcia, C. D. and Carrilho, E. 2014. Determination of nitrite in saliva using microfluidic paper-based analytical devices. *Analytica chimica acta*, 809: 117-122.

Busa, L. S. A. 2016. Development of Microfluidic Paper-based Devices for Food Analysis. PhD, Hokkaido University,

Busa, L. S. A., Mohammadi, S., Maeki, M., Ishida, A., Tani, H. and Tokeshi, M. 2016. Advances in microfluidic paper-based analytical devices for food and water analysis. *Micromachines*, 7 (5): 86.

Britz, A., Gawelda, W., Assefa, T.A., Jamula, L.L., Yarranton, J.T., Galler, A., Khakhulin, D., Diez, M., Harder, M., Doumy, G. and March, A.M., 2019. Using ultrafast X-ray spectroscopy to address questions in ligand-field theory: The excited state spin and structure of [Fe (dcpp) 2] 2+. *Inorganic chemistry*, *58*(14): 9341-9350

Calo, R. and Rosenblat, A. 2017. The taking economy: Uber, information, and power. *Colum. L. Rev.*, 117: 1623.

Cassim, Z. 2018. Cape Town could be the first major city in the world to run out of water. *USA Today* (online) Available: https://www.usatoday.com/story/news/world/2018/01/19/cape-town-could-first-major-city-run-out-water/1047237001/ (Accessed May 26, 2018).

Cate, D. M., Adkins, J. A., Mettakoonpitak, J. and Henry, C. S. 2014. Recent developments in paper-based microfluidic devices. *Analytical chemistry*, 87 (1): 19-41.

Clifton, B. 2012. *Advanced web metrics with Google Analytics*. John Wiley & Sons.

Cosgrove, W. J. and Loucks, D. P. 2015. Water management: Current and future challenges and research directions. *Water Resources Research*, 51 (6): 4823-4839.

Cosgrove, W. J. and Rijsberman, F. R. 2014. *World water vision: making water everybody's business*. Routledge.

Damaceanu, M.-D., Sava, I. and Constantin, C.-P. 2016. The chromic and electrochemical response of CoCl2− filled polyimide materials for sensing applications. *Sensors and Actuators B: Chemical*, 234: 549-561.

Doumit, J. and Lynch Jr, R. J. 2003. *Early warning water leak detection system*: Google Patents.

du Plessis, A. 2017. A Future Outlook: Improved Water Efficiency and Possible Strategic Actions for South Africa and the Upper Vaal WMA. In: *Freshwater Challenges of South Africa and its Upper Vaal River*. Springer, 129-151.

Dungchai, W., Chailapakul, O. and Henry, C. S. 2009. Electrochemical detection for paper-based microfluidics. *Analytical chemistry*, 81 (14): 5821-5826.

Einstein, M. 2016. *Black ops advertising: Native ads, content marketing, and the covert world of the digital sell*. OR Books.

Farley, M., Water, S., Supply, W., Council, S. C. and Organization, W. H. 2001. *Leakage management and control: A best practice training manual*. Geneva: World Health Organization.

Fitzpatrick, D. E., Battilocchio, C. and Ley, S. V. 2016. Enabling technologies for the future of chemical synthesis. *ACS central science*, 2 (3): 131-138.

Gupta, S., Sheikh, M., Islam, M., Rahman, K., Jahan, N., Rahman, M., Hoekstra, R., Johnston, R., Ram, P. and Luby, S. 2008. Usefulness of the hydrogen sulfide test for

assessment of water quality in Bangladesh. *Journal of applied microbiology*, 104 (2): 388-395.

Hasanzadeh, M. and Shadjou, N. 2016. Electrochemical and photoelectrochemical nano-immunesensing using origami paper based method. *Materials Science and Engineering: C*, 61: 979-1001.

Hassan, M. H. A. and Syaza, A. 2018. Review on Microfluidic Paper Based Analytical Devices (μPADs) and Possible Application by Employing Waste Paper. *Journal of Fatwa Management and Research*: 701-715.

Hay, E., Riemann, K., Van Zyl, G. and Thompson, I. 2012. Ensuring water supply for all towns and villages in the Eastern Cape and Western Cape Provinces of South Africa. *Water SA*, 38 (3): 437-444.

Heath, S. 2014. *System and method for using global location information, 2D and 3D mapping, social media, and user behavior and information for a consumer feedback social media analytics platform for providing analytic measurements data of online consumer feedback for global brand products or services of past, present or future customers, users, and/or target markets*: Google Patents.

Hill, N. P. and Sullivan, D. M. 2008. *Touch sensitive device employing impulse reconstruction*: Google Patents.

Hossain, A., Canning, J., Ast, S., Rutledge, P. J., Yen, T. L. and Jamalipour, A. 2015. Lab-in-a-phone: smartphone-based portable fluorometer for pH measurements of environmental water. *IEEE Sensors Journal*, 15 (9): 5095-5102.

Jayawardane, B. M., McKelvie, I. D. and Kolev, S. D. 2015. Development of a gas-diffusion microfluidic paper-based analytical device (μPAD) for the determination of ammonia in wastewater samples. *Analytical chemistry*, 87 (9): 4621-4626.

Jin, S.-Q., Guo, S.-M., Zuo, P. and Ye, B.-C. 2015. A cost-effective Z-folding controlled liquid handling microfluidic paper analysis device for pathogen detection via ATP quantification. *Biosensors and Bioelectronics*, 63: 379-383.

Jokerst, J. C., Adkins, J. A., Bisha, B., Mentele, M. M., Goodridge, L. D. and Henry, C. S. 2012. Development of a paper-based analytical device for colorimetric detection of select foodborne pathogens. *Analytical chemistry*, 84 (6): 2900-2907.

Kang, J., Colanduoni, J. A., Lee, D. J., Youn, B., Ok, C. and Kang, W. J. 1997. *Dipstick immunoassay device*: Google Patents.

Kates, L. 2007. *Method and apparatus for detecting water leaks*: Google Patents.

Kato Jr, E. T., Yoshida, C. M., Reis, A. B., Melo, I. S. and Franco, T. T. 2011. Fast detection of hydrogen sulfide using a biodegradable colorimetric indicator system. *Polymer International*, 60 (6): 951-956.

Kim, S. C., Jalal, U. M., Im, S. B., Ko, S. and Shim, J. S. 2017. A smartphone-based optical platform for colorimetric analysis of microfluidic device. *Sensors and Actuators B: Chemical*, 239: 52-59.

Komatsu, T., Mohammadi, S., Busa, L. S. A., Maeki, M., Ishida, A., Tani, H. and Tokeshi, M. 2016. Image analysis for a microfluidic paper-based analytical device using the CIE L* a* b* color system. *Analyst*, 141 (24): 6507-6509.

Lim, W. Y., Goh, B. T. and Khor, S. M. 2017. Microfluidic paper-based analytical devices for potential use in quantitative and direct detection of disease biomarkers in clinical analysis. *Journal of Chromatography B*, 1060: 424-442.

Liu, L., Yang, D. and Liu, G. 2019. Signal amplification strategies for paper-based analytical devices. *Biosensors and Bioelectronics*,

Liu, S., Su, W. and Ding, X. 2016. A review on microfluidic paper-based analytical devices for glucose detection. *Sensors*, 16 (12): 2086.

Liu, W., Guo, Y., Luo, J., Kou, J., Zheng, H., Li, B. and Zhang, Z. 2015. A molecularly imprinted polymer based a lab-on-paper chemiluminescence device for the detection of dichlorvos. *Spectrochimica Acta Part A: Molecular and Biomolecular Spectroscopy*, 141: 51-57.

Lu, S.Attorney, Agent, or Firm – H. John Rizvi, Gold & RZvi P.A. . 2014. *CENTRALIZED WATER LEAK DETECTION*. USA patent, US 8,922,379 B1

Mayer, J. R. and Mitchell, J. C. 2012. Third-party web tracking: Policy and technology. In: Proceedings of *2012 IEEE symposium on security and privacy*. IEEE, 413-427.

McCrady, E. 1995. pH pens and chlorophenol red. *Alkaline Paper Advocate, The Abbey Newsletter*,

McLaren, K. 1976. XIII—The development of the CIE 1976 (L* a* b*) uniform colour space and colour-difference formula. *Journal of the Society of Dyers and Colourists*, 92 (9): 338-341.

Meredith, N. A., Quinn, C., Cate, D. M., Reilly, T. H., Volckens, J. and Henry, C. S. 2016. based analytical devices for environmental analysis. *Analyst*, 141 (6): 1874-1887.

Meyer, J. 2016. *Water leak detection system*: Google Patents.

Meyer, M. 2017. *eThekwini's R700 million drought-time water loss is worsening a crisis* (online). KwaZulu Natal: Democratic Alliance. Available: http://www.dakzn.org.za/ethekwinis-r700-million-drought-time-water-loss-is-worsening-a-crisis/ (Accessed May 26, 2018).

Mills, A. and Skinner, G. A. 2011. A novel 'fizziness' indicator. *Analyst*, 136 (5): 894-896.

Mosley, L. M. and Sharp, D. S. 2005. The hydrogen sulphide (H2S) paper-strip test. *A simple test for monitoring drinking water quality in the Pacific Islands. South Pacific Applied Geoscience Commission (SOPAC) Technical Report*, 373

Mthembu, C. L., Sabela, M. I., Mlambo, M., Madikizela, L. M., Kanchi, S., Gumede, H. and Mdluli, P. S. 2017. Google Analytics and quick response for advancement of gold nanoparticle-based dual lateral flow immunoassay for malaria–Plasmodium lactate dehydrogenase (pLDH). *Analytical Methods*, 9 (41): 5943-5951.

Nxumalo, N. L. 2019. Development of paper-based microfluidic strips for quantification of ammonia. Masters Dissertation, Durban University of Technology.

Oh, J.-M. and Chow, K.-F. 2015. Recent developments in electrochemical paper-based analytical devices. *Analytical Methods*, 7 (19): 7951-7960.

Pfister, S., Boulay, A.-M., Berger, M., Hadjikakou, M., Motoshita, M., Hess, T., Ridoutt, B., Weinzettel, J., Scherer, L. and Döll, P. 2017. Understanding the LCA and ISO water footprint: A response to Hoekstra (2016)“A critique on the water-scarcity weighted water footprint in LCA”. *Ecological Indicators*, 72: 352-359.

Puust, R., Kapelan, Z., Savic, D. and Koppel, T. 2010. A review of methods for leakage management in pipe networks. *Urban Water Journal*, 7 (1): 25-45.

Rattanarat, P., Dungchai, W., Cate, D. M., Siangproh, W., Volckens, J., Chailapakul, O. and Henry, C. S. 2013. A microfluidic paper-based analytical device for rapid quantification of particulate chromium. *Analytica chimica acta*, 800: 50-55.

Ríos, Á., Zougagh, M. and Avila, M. 2012. Miniaturization through lab-on-a-chip: Utopia or reality for routine laboratories? A review. *Analytica chimica acta*, 740: 1-11.

Rouillard, J. 2008. Contextual QR codes. In: Proceedings of *2008 The Third International Multi-Conference on Computing in the Global Information Technology (iccgi 2008)*. IEEE, 50-55.

Saha, U. and Mukherjea, K. K. 2015. Development of a multifunctional biomimicking L-cysteine based oxovanadium (IV) complex: synthesis, DFT calculations, bromo-peroxidation and nuclease activity. *RSC Advances*, 5 (114): 94462-94473.

Sandhya, K. and Kakulapati, V. 2018. Establishing Secured Enterprise Network Routing protocols by using DMVPN. *International Journal of Computer Science and Information Security (IJCSIS)*, 16 (8)

Seyoum, S., Alfonso, L., van Andel, S. J., Koole, W., Groenewegen, A. and van de Giesen, N. 2017. A Shazam-like household water leakage detection method. *Procedia Engineering*, 186: 452-459.

Shen, Z. 2003. Colour differentiation in digitial images. Victoria University of Technology.

Songjaroen, T., Dungchai, W., Chailapakul, O., Henry, C. S. and Laiwattanapaisal, W. 2012. Blood separation on microfluidic paper-based analytical devices. *Lab on a Chip*, 12 (18): 3392-3398.

The Merck Index, 7th edition, Merck & Co, Rahway, New Jersey, USA, 1960.

Walsh, A. 2010. QR Codes–using mobile phones to deliver library instruction and help at the point of need. *Journal of information literacy*, 4 (1): 55-65.

Wells, A. F. 1984. *Structural Inorganic Chemistry.* 5th ed. Oxford: Clarendon Press

Wu, B. and Xiong, Y. 2013. *System and Method for Mobile Device-Based Smart Wallet*: Google Patents.

Xia, Y., Si, J. and Li, Z. 2016. Fabrication techniques for microfluidic paper-based analytical devices and their applications for biological testing: A review. *Biosensors and Bioelectronics*, 77: 774-789.

Xu, Y., Liu, M., Kong, N. and Liu, J. 2016. Lab-on-paper micro-and nano-analytical devices: fabrication, modification, detection and emerging applications. *Microchimica Acta*, 183 (5): 1521-1542.

Yazdekhasti, S., Piratla, K. R., Matthews, J. C., Khan, A. and Atamturktur, S. 2018. Optimal selection of acoustic leak detection techniques for water pipelines using multi-criteria decision analysis. *Management of Environmental Quality: An International Journal*, 29 (2): 255-277.

Yusufu, D. and Mills, A. 2018. Spectrophotometric and Digital Colour Colourimetric (DCC) analysis of colour-based indicators. *Sensors and Actuators B: Chemical*, 273: 1187-1194.

Appendix

pH	Test
3	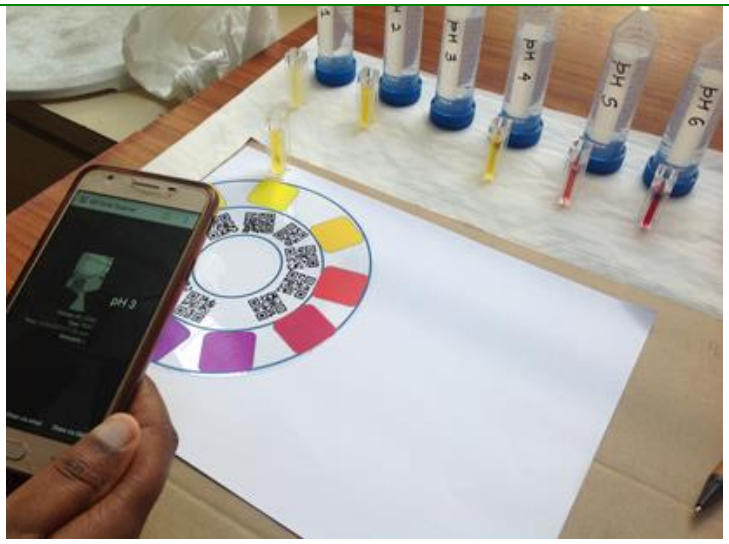
4	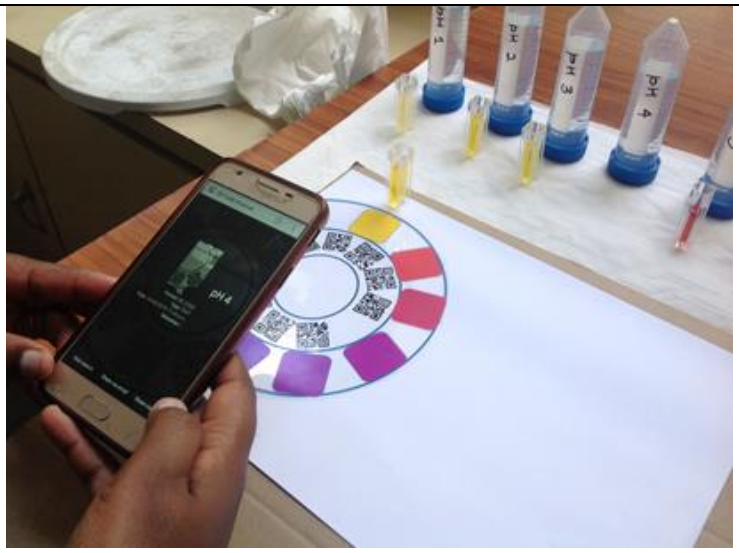

5	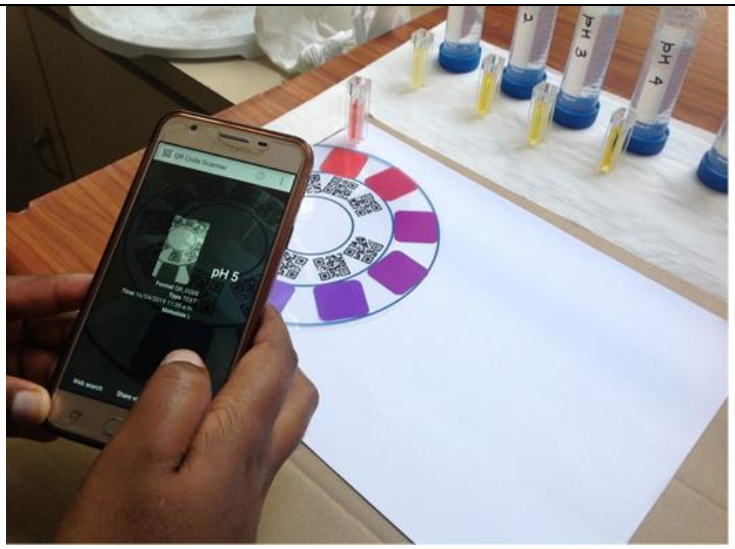 pH 5 pH 3 pH 4
6	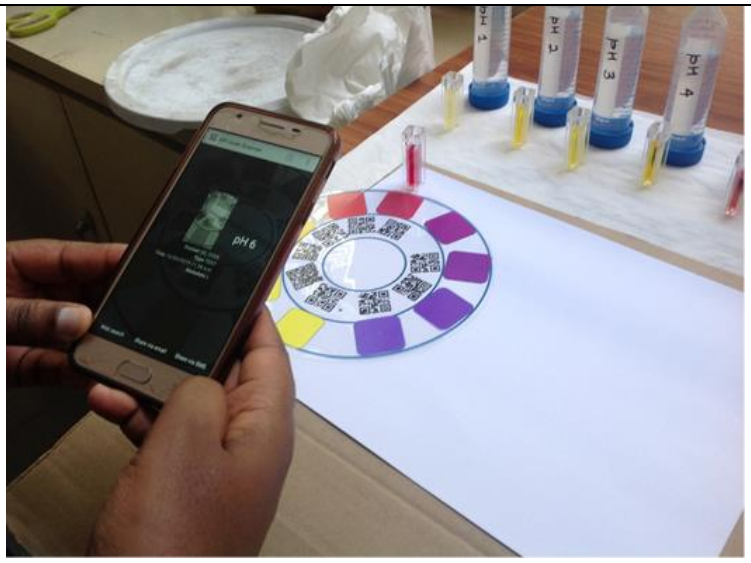 pH 6 pH 1 pH 2 pH 3 pH 4
7	 pH 1 pH 2 pH 3 pH 4 pH 5

8	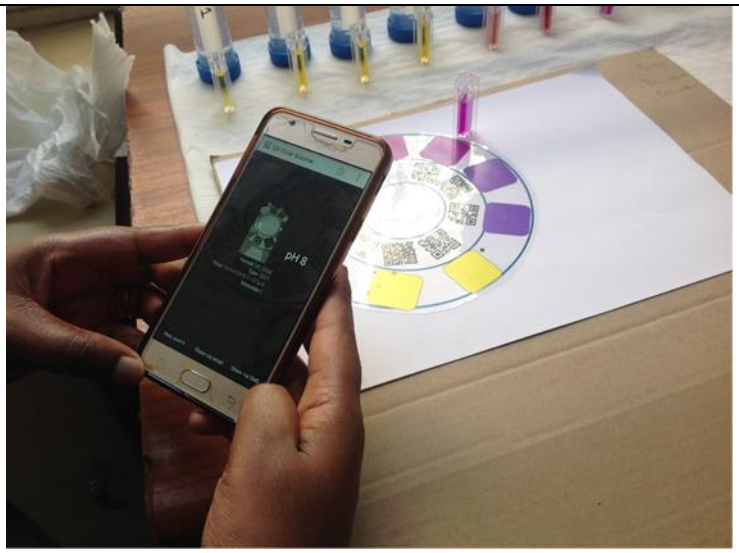
10	

Figure A1: Smartphone recording of colour change

pH	Test
3	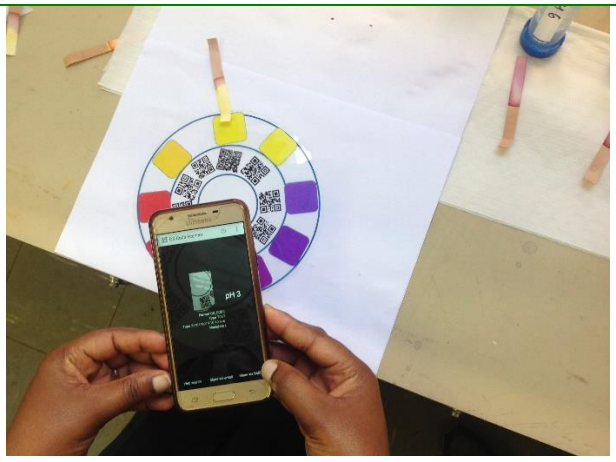

4	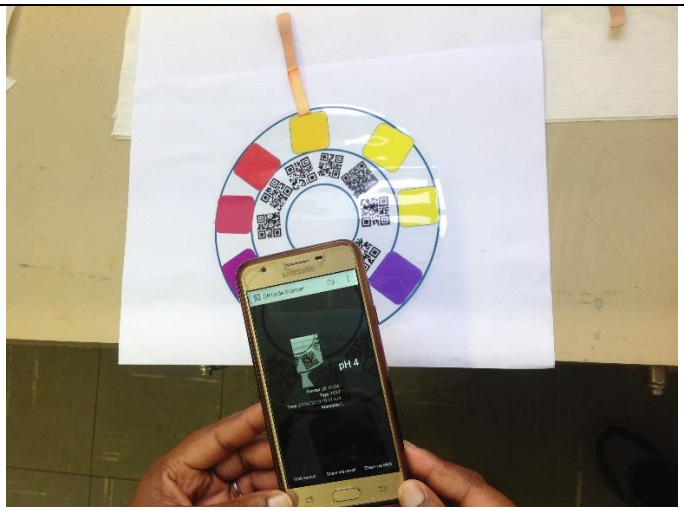
5	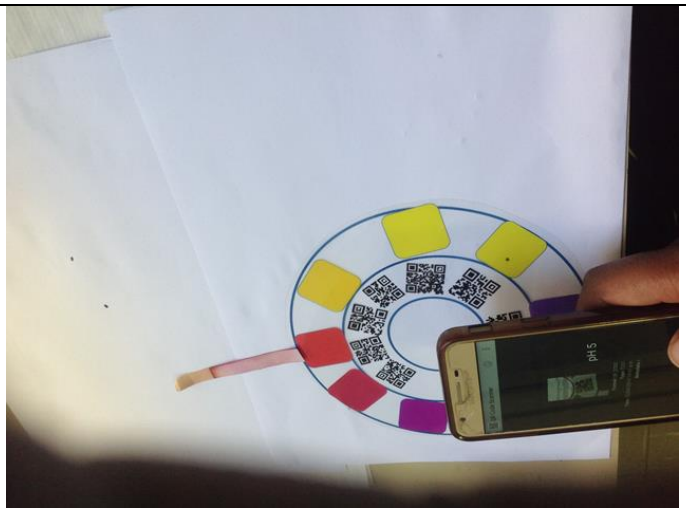
7	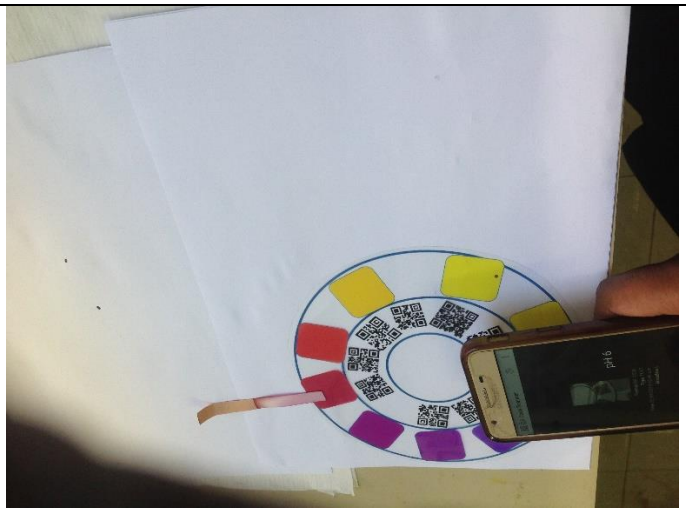

8	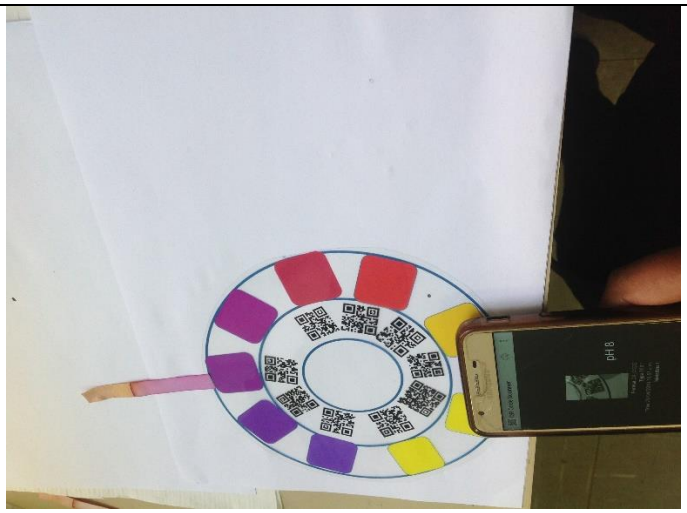
10	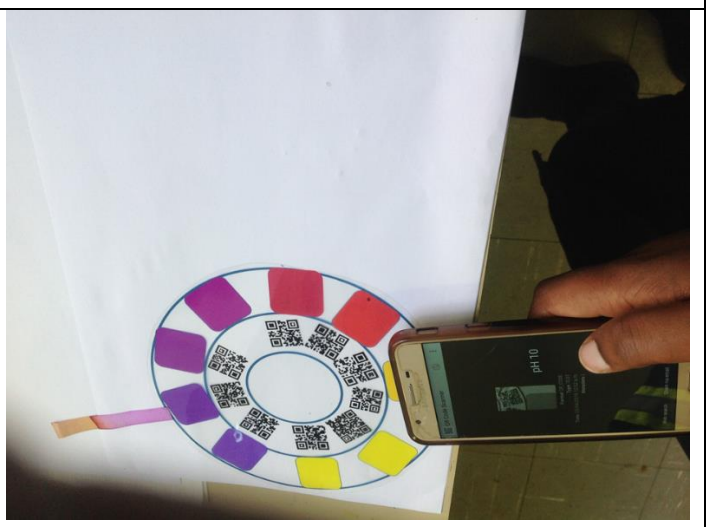

Figure A2: Visual capturing of microfluidic device

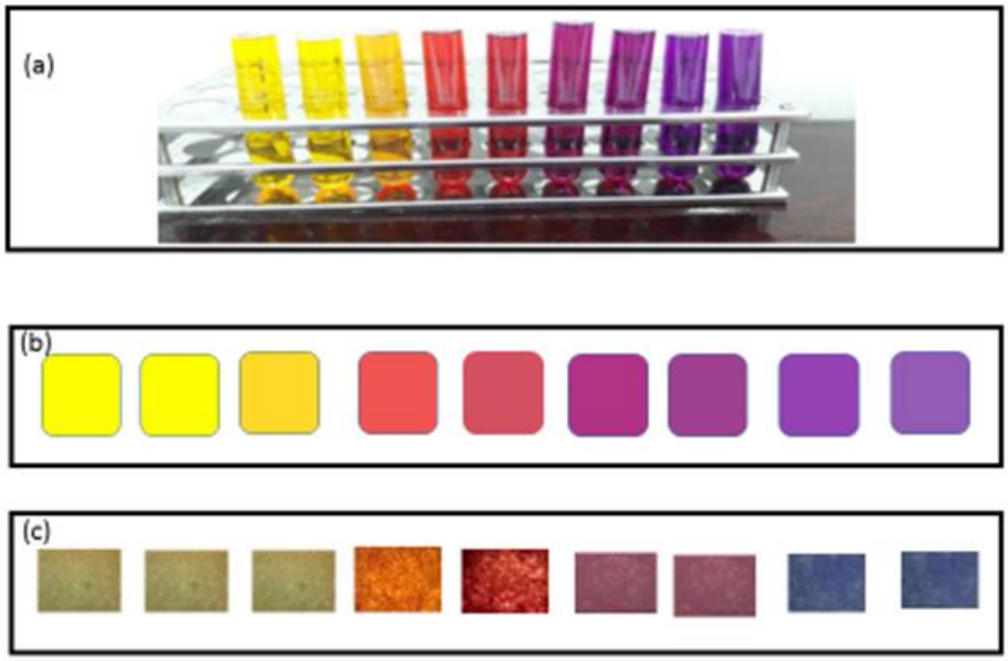

Figure A3: Dried Chlorophenol red test strips (a) cuvette (b) paper (c) optical microscope

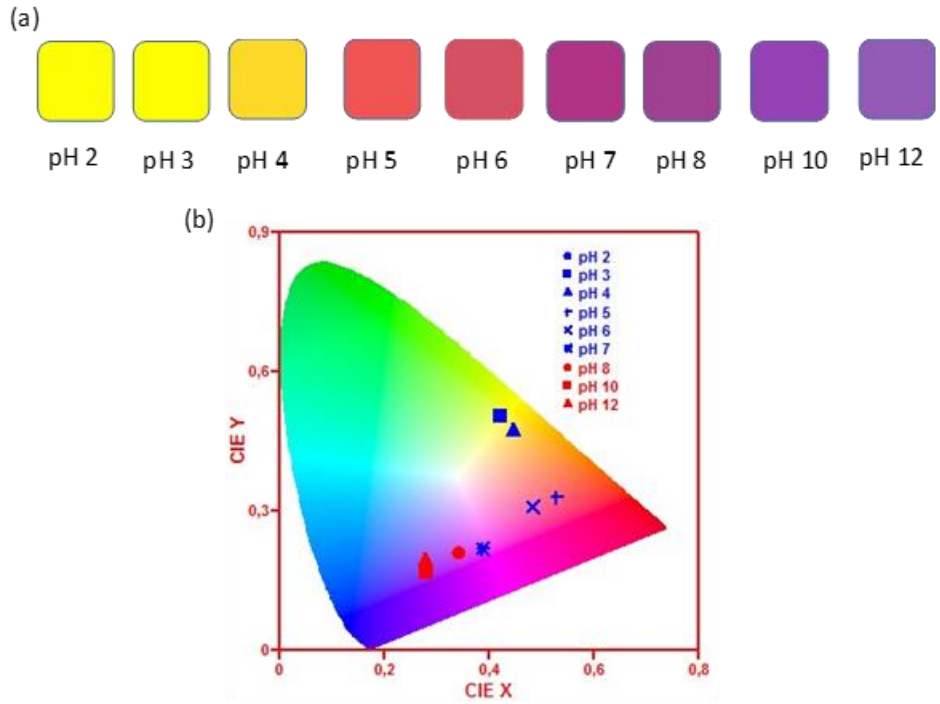

Figure A4: Chlorophenol red test strips (a) RGB; and (b) CIElab

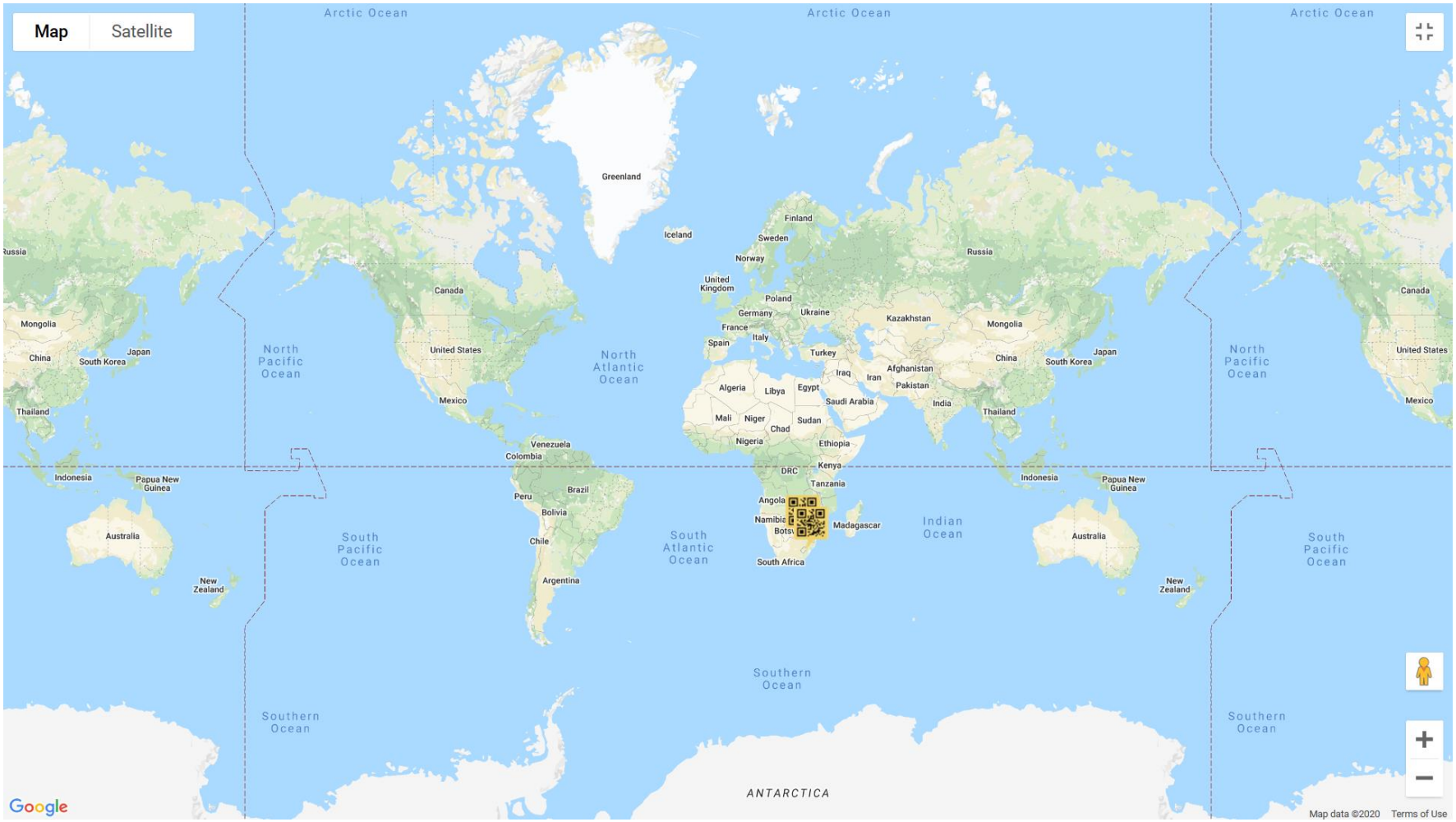

Figure A5 : Map showing the studied area generated by online tracked QR barcodes

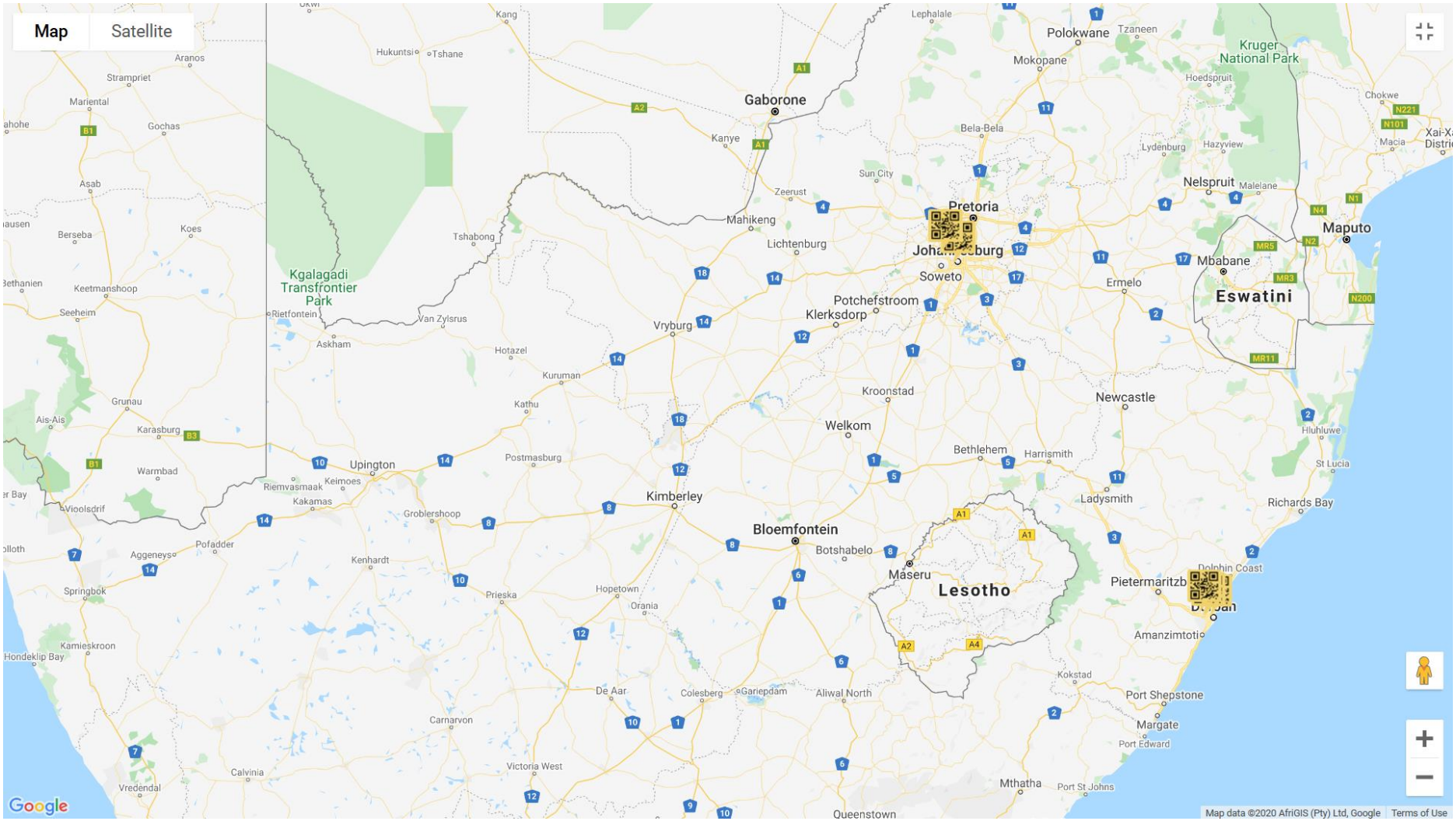

Figure A6: Focal zooming of the tracked QR bacode of the secific focal area of this study

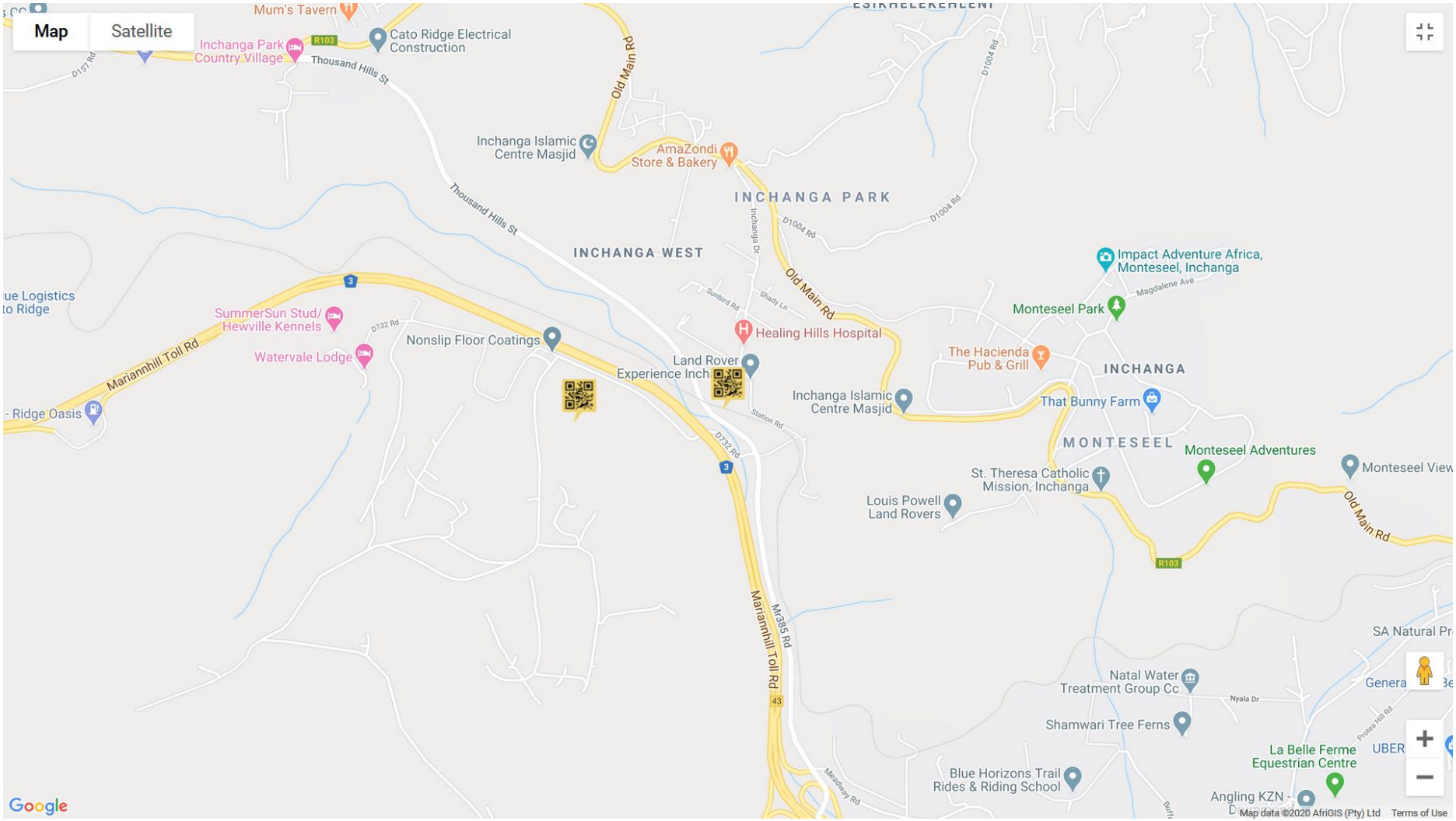

Figure A7: Map shoiwing picture generated from tracked QR barcodes, map can be zoomed to a focal point of interest

Figure A 8 : Zoomed map of the street where a QR bacode was scanned as indication of water leaks.

Table A1: Geolocation Data

Date taken	Time	Device and geolocation points	Place
04/08/2020	06:37:08	Huawei P10 Chrome Mobile 80 (Android 9) Lng/Lat: 31.0449, -29.8556 (accuracy: 100 kilometre)	South Africa KwaZulu-Natal, Durban
04/07/2020	13:13:41	Huawei Mate 20 Pro Chrome Mobile 80 (Android 10) Lng/Lat: 31.0191, -29.8523 (accuracy: 200 kilometre)	South Africa KwaZulu-Natal, Durban
04/07/2020	13:12:28	Huawei Mate 20 Pro Chrome Mobile 80 (Android 10) Access to position was denied by user	South Africa KwaZulu-Natal, Durban
04/07/2020	13:08:25	Huawei Mate 20 Pro Chrome Mobile 80 (Android 10) Lng/Lat: 31.0191, -29.8523 (accuracy: 200 kilometre)	South Africa KwaZulu-Natal, Durban
04/07/2020	13:07:01	Huawei Mate 20 Pro Chrome Mobile 80 (Android 10) Access to position was denied by user	South Africa KwaZulu-Natal, Durban
04/07/2020	11:28:34	LG G5 Chrome Mobile 70 (Android 8.0.0) Lng/Lat: 31.0449, -29.8556 (accuracy: 50 kilometre)	South Africa KwaZulu-Natal, Durban

04/07/2020	11:27:51	LG G5 Chrome Mobile 70 (Android 8.0.0) Inchanga Dr 2 3706 Inchanga Lng/Lat: 30.6629, -29.7418 (accuracy: 1.3 kilometre)	South Africa KZN, Inchanga
04/07/2020	10:35:04	LG G5 Chrome Mobile 70 (Android 8.0.0) D732 Rd 3706 Inchanga Lng/Lat: 30.6561, -29.7423 (accuracy: 3 kilometre)	South Africa KZN, Inchanga
04/07/2020	10:34:06	PC Chrome 80 (Windows 10) Lng/Lat: 28.0583, -26.2309 (accuracy: 1000 kilometre)	South Africa Gauteng, Johannesburg
04/07/2020	10:30:29	LG G5 Chrome Mobile 70 (Android 8.0.0) Lng/Lat: 31.0449, -29.8556 (accuracy: 50 kilometre)	South Africa KwaZulu-Natal, Durban
04/07/2020	10:30:04	LG G5 Chrome Mobile 70 (Android 8.0.0) D732 Rd 3706 Inchanga Lng/Lat: 30.6561, -29.7423 (accuracy: 3 kilometre)	South Africa KZN, Inchanga

04/07/2020	10:28:35	LG G5 Chrome Mobile 70 (Android 8.0.0) D732 Rd 3706 Inchanga Lng/Lat: 30.6561, -29.7423 (accuracy: 3 kilometre)	South Africa KZN, Inchanga
04/07/2020	10:28:09	LG G5 Chrome Mobile 70 (Android 8.0.0) Lng/Lat: 31.0449, -29.8556 (accuracy: 50 kilometre)	South Africa KwaZulu-Natal, Durban
04/07/2020	10:27:19	LG G5 Chrome Mobile 70 (Android 8.0.0) D732 Rd 3706 Inchanga Lng/Lat: 30.6561, -29.7423 (accuracy: 3 kilometre)	South Africa KZN, Inchanga
04/07/2020	09:57:16	LG G5 Chrome Mobile 70 (Android 8.0.0) D732 Rd 3706 Inchanga Lng/Lat: 30.6561, -29.7423 (accuracy: 3 kilometre)	South Africa KZN, Inchanga
04/07/2020	09:21:00	Huawei Y7 (2019) Chrome Mobile 80 (Android 8.1.0) Lng/Lat: 27.9058, -26.1138 (accuracy: 256 meters)	South Africa Gauteng, Johannesburg

04/07/2020	09:20:51	Huawei Y7 (2019) Chrome Mobile 80 (Android 8.1.0) Lng/Lat: 28.0583, -26.2309 (accuracy: 200 kilometre)	South Africa Gauteng, Johannesburg
04/07/2020	09:20:42	Huawei Y7 (2019) Chrome Mobile 80 (Android 8.1.0) Lng/Lat: 27.9058, -26.1138 (accuracy: 256 meters)	South Africa Gauteng, Johannesburg
04/07/2020	09:20:33	Huawei Y7 (2019) Chrome Mobile 80 (Android 8.1.0) Lng/Lat: 28.0583, -26.2309 (accuracy: 200 kilometre)	South Africa Gauteng, Johannesburg
04/07/2020	09:20:22	Huawei Y7 (2019) Chrome Mobile 80 (Android 8.1.0) Lng/Lat: 27.9058, -26.1138 (accuracy: 256 meters)	South Africa Gauteng, Johannesburg